

## CACHEXIA

# Perturbed BMP signaling and denervation promote muscle wasting in cancer cachexia

Roberta Sartori<sup>1,2,3†</sup>, Adam Hagg<sup>1,4,5†</sup>, Sandra Zampieri<sup>3,6,7‡</sup>, Andrea Armani<sup>2,3‡</sup>, Catherine E. Winbanks<sup>1‡</sup>, Laís R. Viana<sup>4,8</sup>, Mouna Haidar<sup>9</sup>, Kevin I. Watt<sup>1,4</sup>, Hongwei Qian<sup>1,4</sup>, Camilla Pezzini<sup>2,3</sup>, Pardis Zanganeh<sup>9</sup>, Bradley J. Turner<sup>9</sup>, Anna Larsson<sup>10</sup>, Gianpietro Zanchetti<sup>6</sup>, Elisa S. Pierobon<sup>6</sup>, Lucia Moletta<sup>6</sup>, Michele Valmasoni<sup>6</sup>, Alberto Ponzoni<sup>11</sup>, Shady Attar<sup>12</sup>, Gianfranco Da Dalt<sup>6</sup>, Cosimo Sperti<sup>6</sup>, Monika Kustermann<sup>13</sup>, Rachel E. Thomson<sup>1,4</sup>, Lars Larsson<sup>14,15,16</sup>, Kate L. Loveland<sup>17,18</sup>, Paola Costelli<sup>19</sup>, Aram Megighian<sup>3</sup>, Stefano Merigliano<sup>6</sup>, Fabio Penna<sup>19</sup>, Paul Gregorevic<sup>1,4,20,21\*§</sup>, Marco Sandri<sup>2,3,7,22\*§</sup>

Most patients with advanced solid cancers exhibit features of cachexia, a debilitating syndrome characterized by progressive loss of skeletal muscle mass and strength. Because the underlying mechanisms of this multifactorial syndrome are incompletely defined, effective therapeutics have yet to be developed. Here, we show that diminished bone morphogenetic protein (BMP) signaling is observed early in the onset of skeletal muscle wasting associated with cancer cachexia in mouse models and in patients with cancer. Cancer-mediated factors including Activin A and IL-6 trigger the expression of the BMP inhibitor Noggin in muscle, which blocks the actions of BMPs on muscle fibers and motor nerves, subsequently causing disruption of the neuromuscular junction (NMJ), denervation, and muscle wasting. Increasing BMP signaling in the muscles of tumor-bearing mice by gene delivery or pharmacological means can prevent muscle wasting and preserve measures of NMJ function. The data identify perturbed BMP signaling and denervation of muscle fibers as important pathogenic mechanisms of muscle wasting associated with tumor growth. Collectively, these findings present interventions that promote BMP-mediated signaling as an attractive strategy to counteract the loss of functional musculature in patients with cancer.

## INTRODUCTION

Cachexia, a multifactorial syndrome characterized by severe wasting of skeletal muscle and fat despite nutritional support, is a common feature of advanced cancer (1, 2). The increasingly debilitating functional impairment of muscle experienced by cachectic individuals increases morbidity and reduces both tolerance and responsiveness to treatment regimens, complicating patient management and ultimately

accounting for up to 30% of deaths associated with advanced cancer (3). Although the pathogenic mechanisms responsible for cancer cachexia remain incompletely defined, the loss of muscle mass and strength is considered the most important clinical feature of cancer cachexia and a key predictor of poor outcomes (4). Preservation of muscle mass independent of fat loss and tumor growth has been shown to extend survival in animal models of cachexia (5). These observations suggest that interventions capable of conserving and/or restoring functional muscle mass offer considerable potential in combination with anticancer regimens to enhance patient outcomes.

Muscle atrophy arises when hyperactivation of proteolysis and organelle degradation exceeds rates of protein synthesis and organelle biogenesis. Proteolysis occurs via calcium-dependent proteolytic pathways (6) and ubiquitin-mediated proteasomal and autophagic lysosomal processes (7) that are potentiated when cellular signaling events promote excessive transcription of genes encoding for rate-limiting enzymes of the degradative systems (8). As a regulator of protein synthesis and degradation processes, the transforming growth factor- $\beta$  (TGF $\beta$ ) network has emerged as one of the most important governors of muscle mass (9–11). Specific TGF $\beta$  family ligands that use Activin receptors (ActRs) and SMAD2/3 second messengers modulate protein turnover in favor of catabolism and have been associated with conditions characterized by muscle atrophy, including cachexia (12–14). Inhibition of ActR-SMAD2/3 signaling has been proposed as a therapeutic for cancer cachexia, after studies reporting improved survival in mice concomitant with preservation of muscle mass despite unchanged tumor growth, fat loss, and proinflammatory cytokine production (5). However, clinical translation has been hampered by the challenges of developing interventions that achieve efficacious targeting of excessive ActR-SMAD2/3 signaling in muscle without side effects in other cell types and tissues (15, 16),

<sup>1</sup>Baker Heart and Diabetes Institute, Melbourne, VIC 3004, Australia. <sup>2</sup>Veneto Institute of Molecular Medicine, 35129 Padova, Italy. <sup>3</sup>Department of Biomedical Sciences, University of Padova, 35131 Padova, Italy. <sup>4</sup>Centre for Muscle Research, Department of Anatomy and Physiology, University of Melbourne, Melbourne, VIC 3010, Australia. <sup>5</sup>Biomedicine Discovery Institute, Department of Physiology, Monash University, Melbourne, VIC 3800, Australia. <sup>6</sup>Department of Surgery, Oncology and Gastroenterology, 3rd Surgical Clinic, University of Padova, 35128 Padua, Italy. <sup>7</sup>Myology Center, University of Padova, 35122 Padua, Italy. <sup>8</sup>Department of Structural and Functional Biology, Biology Institute, University of Campinas, Campinas, São Paulo 13083-97, Brazil. <sup>9</sup>The Florey Institute of Neuroscience and Mental Health, Parkville, VIC 3052, Australia. <sup>10</sup>Theme Cancer, Karolinska University Hospital, Solna 171 76, Sweden. <sup>11</sup>Department of Radiology, Padova General Hospital, 35121 Padova, Italy. <sup>12</sup>Department of Medicine, University Hospital of Padova, 35121 Padova, Italy. <sup>13</sup>Center for Anatomy and Cell Biology, Medical University of Vienna, 1090 Vienna, Austria. <sup>14</sup>Department of Physiology and Pharmacology, Karolinska Institutet, 171 77 Stockholm, Sweden. <sup>15</sup>Department of Clinical Neuroscience, Karolinska Institutet, 171 77 Stockholm, Sweden. <sup>16</sup>Department of Biobehavioral Health, The Pennsylvania State University, University Park, PA 16802, USA. <sup>17</sup>Centre for Reproductive Health, Hudson Institute of Medical Research, Clayton, VIC 3168, Australia. <sup>18</sup>Department of Molecular and Translational Sciences, and Anatomy and Developmental Biology, Monash University, VIC 3800, Australia. <sup>19</sup>Department of Clinical and Biological Sciences, University of Turin, 10125 Turin, Italy. <sup>20</sup>Department of Biochemistry and Molecular Biology, Monash University, VIC 3800, Australia. <sup>21</sup>Department of Neurology, University of Washington School of Medicine, Seattle, WA 98195, USA. <sup>22</sup>Department of Medicine, McGill University, Montreal, QC H4A 3J1, Canada.

\*Corresponding author. Email: pgre@unimelb.edu.au (P.G.); marco.sandri@unipd.it (M.S.)

†These authors contributed equally to this work.

‡These authors contributed equally to this work.

§These authors contributed equally to this work.

highlighting the need to investigate alternative strategies to combat the muscle weakness underlying cachexia.

Recent studies have independently identified that the bone morphogenetic protein (BMP) pathway operates in parallel, and in opposition, to ActR-SMAD2/3 signaling as a vital positive regulator of muscle mass (17, 18). The BMP pathway performs an essential role in mitigating proteolysis by repressing the transcription of atrophy-associated E3 ubiquitin ligases that facilitate proteasome-dependent protein breakdown, including MUSA1 (Muscle Ubiquitin ligase of the SCF complex in Atrophy-1) (*Fbxo30*) (17, 18). Because the experimental inhibition of BMP signaling in mouse models of nutritional deficit and neurogenic atrophy provokes exacerbated muscle wasting and weakness reminiscent of that associated with advanced cachexia (17, 18), we reasoned that perturbation of BMP signaling in muscle may be implicated in the etiology of cancer cachexia. The BMP pathway has also been identified as a regulator of neuromuscular junction (NMJ) formation and remodeling during insect development (19–21). Consequently, we hypothesized that perturbation of BMP signaling in adult mammalian musculature could contribute to the development of defects in the interaction between motor nerves and muscle fibers via the NMJ, with deleterious consequences for regulation of muscle mass and function. From studies examining mouse models of cancer cachexia, we report data that identify markedly diminished BMP signaling and disruption of NMJ architecture, leading to myofiber denervation as events underlying muscle wasting associated with cachexia due to advanced cancer. Moreover, comparing the preclinical data with those obtained from biopsies and blood samples from patients with cachexia-inducing cancers, we suggest that similar BMP signaling and NMJ alterations might also be present in patients.

## RESULTS

### BMP signaling in muscle is down-regulated in models of cancer cachexia, and restoring BMP activity ameliorates cancer-mediated muscle wasting

Because the genetic or pharmacological inhibition of BMP-SMAD1/5/8 signaling exacerbates muscle atrophy under catabolic conditions such as fasting and denervation (17, 18), we examined the phosphorylation of SMAD1/5/8 (p-SMAD1/5/8) as a measure of BMP pathway activation in the muscles of C26 tumor-bearing mice, as an established model of cancer cachexia (22). We found that the tibialis anterior (TA) and the gastrocnemius (GAS) hindlimb muscles of cachectic mice displayed a down-regulation of p-SMAD1/5/8 compared to the muscles of controls (Fig. 1A and fig. S1A). To confirm the depression of BMP-SMAD1/5/8 signaling in cachectic muscles, we purified nuclei from the TA muscles of additional cohorts of tumor-bearing and control mice and observed a decreased nuclear abundance of p-SMAD1 in cachectic mice (fig. S1B). A time course analysis revealed that nuclear p-SMAD1/5/8 content was reduced early in the manifestation of cancer-induced muscle atrophy and as cachexia progressed (fig. S1C). p-SMAD3 was increased in the muscles of tumor-bearing mice early in the time course of cachexia development but not during the ensuing stages of muscle wasting (fig. S1, D to F). As a marker of perturbed BMP-SMAD1/5/8 signaling in cancer cachexia, we examined the expression of the E3 ubiquitin ligase *Fbxo30* (MUSA1), a bona fide downstream target that is repressed by p-SMAD1/5/8 (17, 18). By comparing the expression of *Fbxo30* (MUSA1) with the other atrophy-related ubiquitin ligases

*Fbxo32* (Atrogin1), *Trim63* (MuRF1, Muscle RING-finger protein-1), and *Fbxo21* (SMART, Specific of Muscle Atrophy and Regulated by Transcription) (23), we observed that *Fbxo30* (MUSA1) was up-regulated in the TA (Fig. 1B) and other muscles of C26 tumor-bearing mice (fig. S2, A to C). Ligands that promote SMAD2/3 signaling constitute one mode by which the actions of endogenous BMPs can be antagonized, increased expression of Noggin, an inhibitor of BMPs, and can also inhibit SMAD1/5/8 signaling, as previously published (24, 25). Accordingly, we found that Noggin (*Nog*) expression was increased in the TA (Fig. 1C) and other muscles of cachectic mice bearing C26 tumors (fig. S2, D and E). Other components of the BMP pathway were also affected in muscle as a consequence of tumor growth. Expression of *Bmp7* was reduced, whereas two other BMP inhibitors, Gremlin1 (*Grem1*) and Chordin (*Chrd*), were up-regulated in cachectic C26 tumor-bearing mice (fig. S3A), and the expression of several different type I and type II BMP receptors was altered in the TA and GAS muscles of cachectic mice (fig. S3, B and C). Collectively, these findings demonstrate that regulatory components of the BMP pathway are modulated in skeletal muscles in mice by processes associated with tumor growth.

To test whether preserving BMP-SMAD1/5/8 signaling can prevent muscle atrophy underlying cachexia, we overexpressed a constitutively active variant of the BMP type I receptor, caBMPRI1A (17), in the limb muscles of C26 tumor-bearing mice. Expression of caBMPRI1A (fig. S4A) in TA muscles maintained p-SMAD1/5/8 abundance (Fig. 1D), preserved the mass of treated muscles (Fig. 1, E and F), and blunted the expression of *Trim63* (MuRF1) and *Fbxo30* (MUSA1) (fig. S4B). As an alternative approach, we tested whether increasing SMAD1/5/8 signaling via overexpression of BMP7 could recapitulate the protective effects associated with caBMPRI1A expression and observed that adeno-associated viral (AAV) vector-mediated overexpression of BMP7 in the TA muscles of C26 tumor-bearing mice (fig. S4C) preserved p-SMAD1/5/8 abundance (Fig. 1G), reduced loss of muscle mass (Fig. 1, H and I), and blunted the expression of *Fbxo30* (MUSA1) (fig. S4D). Because MUSA1 is a driver of protein degradation that is negatively regulated by p-SMAD1/5/8 and induced in cachectic muscles (fig. S5A), we determined its contribution to cachexia using a loss-of-function approach. Consistent with the data that MUSA1 is downstream of BMP signaling, inhibition of MUSA1 by RNA interference (fig. S5B) ameliorated the loss of muscle mass in C26 tumor-bearing mice (Fig. 1J).

To establish whether BMP signaling is diminished in other established animal models of cachexia, we examined the muscles of inhibin- $\alpha$  null mice (*Inha*<sup>-/-</sup>), which develop cachexia subsequent to formation of gonadal tumors (fig. S6, A and B) (26). Consistent with our observations of C26 tumor-bearing mice, we observed that BMP signaling is also reduced in the muscles of cachectic *Inha*<sup>-/-</sup> mice when compared to control mice (fig. S6C) and was associated with increased *Fbxo30* (MUSA1) gene expression (fig. S6D), *Nog* (fig. S6E). Moreover, as with the C26 tumor-bearing mice treated with AAV:BMP7, we observed that BMP7 overexpression in the TA muscles of *Inha*<sup>-/-</sup> mice maintained p-SMAD1/5/8 abundance (fig. S6F) and attenuated muscle wasting (fig. S6, G and H). Because the loss of body mass in C26 tumor-bearing mice and *Inha*<sup>-/-</sup> mice has been associated with elevated circulating concentrations of Activin A (26, 27) and as Activin A is sufficient to cause muscle wasting independently of tumor development and progression (14, 27), we investigated the effect of Activin A overexpression on BMP pathway activity. Using AAV vector-mediated gene delivery,

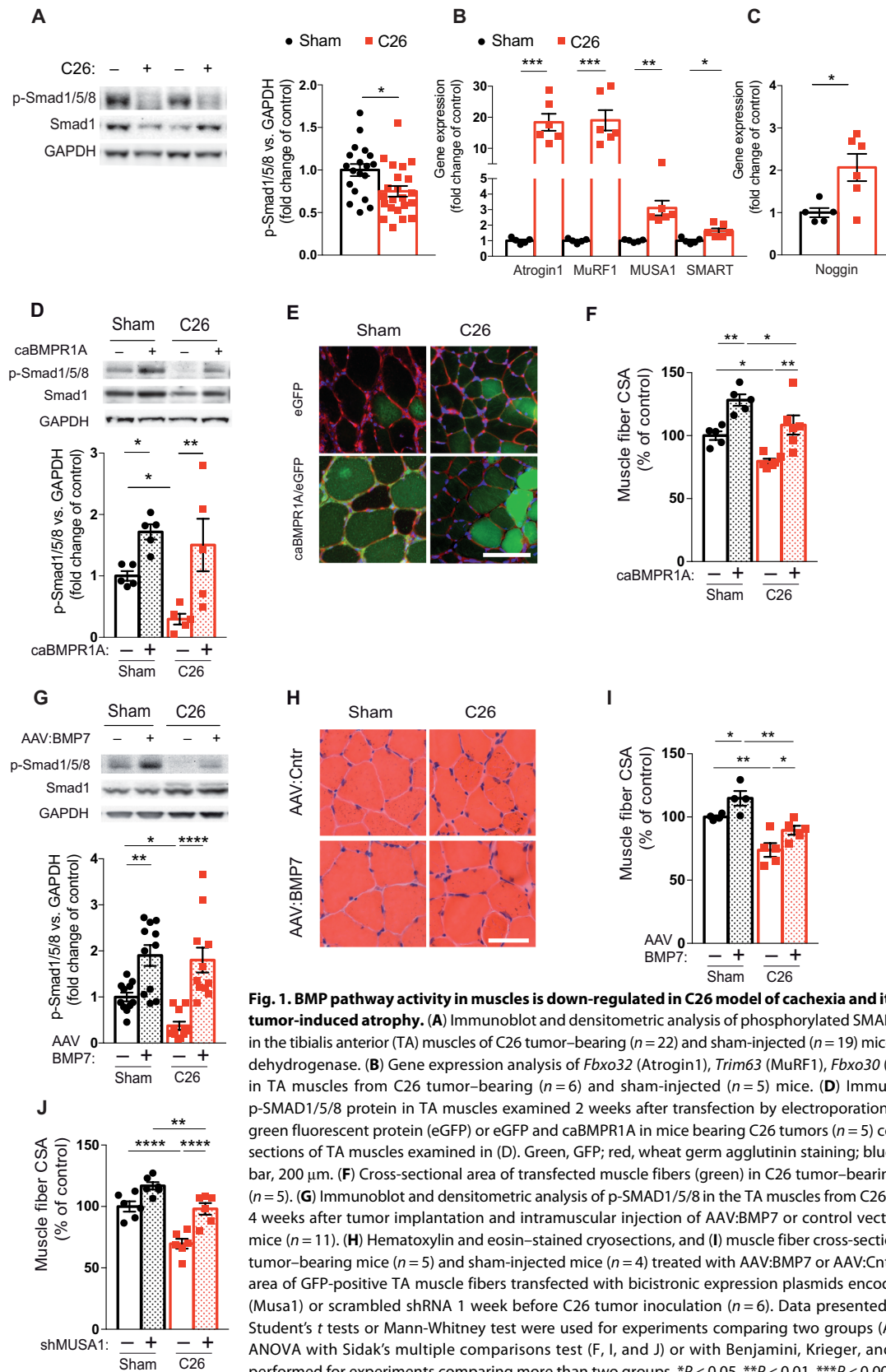


**Fig. 1. BMP pathway activity in muscles is down-regulated in C26 model of cachexia and its reactivation protects muscles from tumor-induced atrophy.** (A) Immunoblot and densitometric analysis of phosphorylated SMAD1/5/8 (p-SMAD1/5/8) protein quantity in the tibialis anterior (TA) muscles of C26 tumor-bearing ( $n = 22$ ) and sham-injected ( $n = 19$ ) mice. GAPDH, glyceraldehyde-3-phosphate dehydrogenase. (B) Gene expression analysis of *Fbxo32* (Atrogin1), *Trim63* (MuRF1), *Fbxo30* (MUSA1), *Fbxo21* (SMART), and (C) *Nog* in TA muscles from C26 tumor-bearing ( $n = 6$ ) and sham-injected ( $n = 5$ ) mice. (D) Immunoblot and densitometric analysis of p-SMAD1/5/8 protein in TA muscles examined 2 weeks after transfection by electroporation with constructs expressing enhanced green fluorescent protein (eGFP) or eGFP and caBMPR1A in mice bearing C26 tumors ( $n = 5$ ) compared with controls ( $n = 5$ ). (E) Cryosections of TA muscles examined in (D). Green, GFP; red, wheat germ agglutinin staining; blue, 4',6-diamidino-2-phenylindole. Scale bar, 200  $\mu$ m. (F) Cross-sectional area of transfected muscle fibers (green) in C26 tumor-bearing mice ( $n = 6$ ) and sham-injected mice ( $n = 5$ ). (G) Immunoblot and densitometric analysis of p-SMAD1/5/8 in the TA muscles from C26 tumor-bearing mice ( $n = 11$ ) examined 4 weeks after tumor implantation and intramuscular injection of AAV:BMP7 or control vector (AAV:Cntr) and from sham-injected mice ( $n = 11$ ). (H) Hematoxylin and eosin-stained cryosections, and (I) muscle fiber cross-sectional area (CSA) of TA muscles from C26 tumor-bearing mice ( $n = 5$ ) and sham-injected mice ( $n = 4$ ) treated with AAV:BMP7 or AAV:Cntr. Scale bar, 200  $\mu$ m. (J) Cross-sectional area of GFP-positive TA muscle fibers transfected with bicistronic expression plasmids encoding eGFP, and shRNAs against *Fbxo30* (Musa1) or scrambled shRNA 1 week before C26 tumor inoculation ( $n = 6$ ). Data presented as means  $\pm$  SEM. Unpaired two-tailed Student's *t* tests or Mann-Whitney test were used for experiments comparing two groups (A to C). A two-way repeated-measures ANOVA with Sidak's multiple comparisons test (F, I, and J) or with Benjamini, Krieger, and Yekutieli adjustment (D and G) was performed for experiments comparing more than two groups. \* $P < 0.05$ , \*\* $P < 0.01$ , \*\*\* $P < 0.001$ , and \*\*\*\* $P < 0.0001$ .

we transduced the TA muscles of adult mice with an inducible Activin A expression vector, which was sufficient to cause a ~40% reduction in muscle mass within 4 weeks of induction (fig. S7A). Activin A-mediated muscle atrophy was associated with decreased p-SMAD1/5/8, increased p-SMAD2 and p-SMAD3 (fig. S7, B to D), and increased expression of *Fbxo30* (MUSA1) (fig. S7E) and *Nog* (fig. S7F). The expression of *Grem1* and *Chrd* was not affected by Activin A overexpression (fig. S7G). In addition, the expression of either caBMPR1A (fig. S7H) (12) or BMP7 (fig. S7I) was associated with amelioration of Activin A-mediated muscle atrophy. The observations across these mouse models demonstrate that signaling via the BMP-SMAD1/5/8 axis is inhibited in settings of muscle atrophy associated with cachexia and that restoring signaling via the BMP-SMAD1/5/8 pathway and/or repression of the SMAD1/5/8 target MUSA1 is beneficial for preservation of muscle mass in settings of cachexia.

### Impaired BMP signaling contributes to NMJ dismantling and myofiber denervation in cachexia

As we have shown that BMP-SMAD1/5/8 signaling is important for conservation of muscle mass when the NMJ is compromised (17, 18), we hypothesized that interactions between motor nerves and muscle fibers may also become compromised in cancer and, therefore, may contribute to muscle atrophy. To test this hypothesis, we immunolabeled the presynaptic and postsynaptic components of the NMJ in various skeletal muscles and used confocal microscopy to assess the morphology of the NMJ. The extensor digitorum longus (EDL) muscles of noncachectic tumor-free mice exhibited normal axon and terminal morphology and consistently colocalized labeling of presynaptic neurofilament/synaptic vesicle and postsynaptic acetylcholine receptors (AChRs) (Fig. 2A). In contrast, EDL muscles from end-stage tumor-bearing mice displayed a notable lack of colocalization between pre- and postsynaptic structures, as well as evidence of motor neuron terminal retraction and degeneration (Fig. 2A), accompanied by reduced peripheral synapse area and volume (Fig. 2, B to D). To determine whether the NMJ degeneration and axon retraction occur before cachexia onset or are a consequence of muscle loss, we examined NMJ morphology across the time course of cachexia. Indices of disrupted presynaptic architecture and NMJ degeneration were observed in the muscles of tumor-bearing mice before muscle loss occurred (T1; Fig. 2E). Quantitative measurements confirmed that up to 60% of NMJs [as identified by labeling with  $\alpha$ -bungarotoxin (BTX)] were affected within the muscles of cachectic mice (T3; Fig. 2E). The number of motor neurons in the lumbar spinal cord did not differ between sham and cachectic mice (Fig. 2F), indicating that the observed NMJ degeneration associated with cachexia is not a consequence of spinal motor neuron loss but likely a product of abnormalities at the peripheral synapse. Defects in NMJ organization were consistently observed in multiple appendicular muscles from tumor-bearing mice, including the TA and GAS (fig. S8, A and B). To confirm the perturbation of NMJ organization, we examined the muscles of tumor-bearing mice for localization of neural cell adhesion molecule (NCAM), which is typically enriched in the postsynaptic endplates of the NMJ but becomes transiently redistributed on the muscle fiber membrane or cytoplasm proximal to the NMJ when innervation is lost (28). Immunofluorescent analyses identified the presence of denervated NCAM-positive fibers in different muscles from mice bearing C26 tumors (fig. S8, C to G), which were predominantly type IIb and IIx by myosin heavy-chain composition (fig. S8, C to G).

Examination of NCAM1 (*Ncam1*), AChR (*Chrnrg*), muscle-associated receptor tyrosine kinase (*Musk*), myogenin (*Myog*), and runt-related transcription factor 1 (*Runx1*) transcription as established markers of denervation and NMJ remodeling (29, 30) demonstrated that most of the markers were up-regulated in different appendicular muscles and axial musculature from mice bearing C26 tumors (Fig. 2G and fig. S9, A to C). To determine the functional relevance of these morphological defects in NMJ organization, we recorded electromyographic responses to sciatic nerve stimulation in the EDL, GAS, and TA muscles of cachectic C26 tumor-bearing mice. Abnormal compound muscle action potentials (CMAPs) were consistently detected in the muscles of C26 tumor-bearing mice (Fig. 2, H to J, and fig. S10, A to F), thereby confirming that muscle fiber innervation and neurotransmission are functionally impaired in muscles rendered cachectic by advanced cancer. Specifically, quantification of electromyographic analyses determined that cachectic muscles of C26 tumor-bearing mice exhibited prolonged and polyphasic CMAP whose amplitude declined after repetitive nerve stimulation at 10 Hz for 20 s compared to muscles of sham mice (Fig. 2, K to M, and fig. S10, A to F). Having identified a mechanism implicating repression of BMP signaling and perturbation of the NMJ as an early step in cancer cachexia, we reasoned that increasing the otherwise perturbed BMP signaling in muscles associated with cancer progression could not only counteract muscle atrophy (Fig. 1, E, F, H, and I) but also prevent the manifestation of NMJ pathology in the setting of cachexia. In C26 tumor-bearing mice, a systemic dose of AAV:BMP7 or AAV:caBMPR1A was sufficient to correct parameters of NMJ function, compared with tumor-bearing mice receiving control vector (Fig. 2, K to M, and fig. S10, G to L).

Having observed that Noggin is up-regulated at the transcript (Fig. 1C) and protein (Fig. 3A) level in cachectic muscles, we sought to establish whether inhibition of the BMP pathway is sufficient to recapitulate the denervation phenotype of tumor-bearing mice. We found that overexpression of Noggin in the muscles of healthy mice (fig. S11, A and B) induced muscle atrophy (Fig. 3, B and C, and fig. S11C) to a greater extent than Chordin overexpression (fig. S11D); induced the expression of *Fbxo32* (Atrogin1), *Trim63* (MuRF1), and *Fbxo30* (MUSA1) (Fig. 3D); recapitulated the loss of presynaptic motor neuron terminals (Fig. 3, E and F); up-regulated the presence of denervation markers (Fig. 3G); induced the appearance of denervated NCAM-positive fibers (fig. S11E); and caused electromyographic patterns that are consistent with denervation such as CMAP alteration and spontaneous myofiber depolarization (Fig. 3, H and I, and fig. S11, F and G). Conversely, Noggin inhibition in mice bearing C26 tumors (fig. S11H) blunted the up-regulation of *Trim63* (MuRF1) (fig. S11I) and largely prevented the up-regulation of genes associated with denervation (fig. S11J). Together, these data demonstrate that tumor growth is associated with increased expression of the BMP inhibitor Noggin in skeletal muscles and that increased Noggin abundance can promote degeneration of the NMJ architecture in healthy mice.

To identify factors that contribute to the up-regulation of Noggin transcription in the muscles of tumor-bearing mice and to establish whether Noggin is linked to cachexia or tumor growth, we inoculated mice with the noncachectic MC38 colon carcinoma cell line (31). Mice developed tumors (Fig. 4A) but did not demonstrate a loss of body mass and muscle mass (Fig. 4B and fig. S12, A and B). Furthermore, the transcription of *Fbxo32* (Atrogin1), *Trim63* (MuRF1), *Fbxo30* (MUSA1) and *Fbxo21* (SMART), *Nog*, and genes associated with denervation was not differentially regulated in the muscles of mice

**Fig. 2. NMJ impairment and denervation in cachexia.**

(A) Labeled presynaptic (neurofilament (2H3); synaptic vesicle (SV2); red) and postsynaptic (bungarotoxin (BTX); green) NMJ components in EDL muscles from C26 tumor-bearing mice and sham-injected mice. Scale bars, 20  $\mu\text{m}$ . (B) NMJ area, (C) volume, and (D) fragmentation in EDL muscles of C26 tumor-bearing mice ( $n = 5$ ) compared to sham-injected mice ( $n = 6$ ). (E) Proportion of innervated (Inn) (green/red label overlap) and denervated (Den) (lack of green/red overlap) NMJs in the EDL muscles during the progression of lean mass (LM) loss. (controls,  $n = 6$ ; C26 T1 and T2,  $n = 6$ ; C26 T3,  $n = 5$ ). (F) Number of motor neurons (MNs) per ventral horn and total number, in the lumbar spinal cord of cachectic mice ( $n = 5$ ) and sham-injected ( $n = 5$ ) mice. (G) Transcription of *Ncam1*, *Musk*, *Myog*, and *Runx1* (genes associated with denervation) is increased in EDL muscles of C26 tumor-bearing mice ( $n = 8$ ) compared to sham-injected mice ( $n = 7$ ). Representative electromyographic traces of abnormal nerve-evoked compound muscle action potentials (CMAPs) detected in (H) the EDL muscles of 5 of 6 C26 tumor-bearing mice compared with sham-injected mice ( $n = 5$ ) in (I) the TA muscles of 9 of 10 C26 tumor-bearing mice compared with sham-injected mice ( $n = 7$ ) and in (J) the GAS muscles of C26 tumor-bearing mice ( $n = 6$ ) compared with control mice ( $n = 6$ ) (arrows indicate stimulus artifacts). (K) CMAP duration from TA muscles of C26 tumor-bearing mice examined 4 weeks after tumor implantation and 5 weeks after systemic administration of AAV:BMP7 ( $n = 13$ ), AAV:caBMPR1A ( $n = 5$ ), or AAV:Cntr ( $n = 9$ ) and control mice ( $n = 5$ ), as recorded after single nerve stimuli delivered at 0.5 Hz. (L) CMAP amplitude decay (percentage of beginning) in the last 5 s after repetitive nerve stimulation at 10 Hz for 20 s from TA muscles of C26 tumor-bearing mice examined 4 weeks after tumor implantation and 5 weeks after systemic administration of AAV:BMP7 ( $n = 10$ ), AAV:caBMPR1A ( $n = 5$ ), or AAV:Cntr ( $n = 5$ ) and control mice ( $n = 5$ ). (M) Proportion (percentage of total) of biphasic (physiological) versus polyphasic (pathological) CMAPs under different experimental conditions showed in (L). Data presented as means  $\pm$  SEM. Unpaired two-tailed Student's *t* tests (B, D, F, and G) or Mann-Whitney test (C and K) were used for experiments comparing two groups. A one-way ANOVA with Tukey multiple comparisons test (E) or with Benjamini, Krieger, and Yekutieli adjustment (L) was performed for experiments comparing more than two groups. \* $P < 0.05$ , \*\* $P < 0.01$ , \*\*\* $P < 0.001$ , and \*\*\*\* $P < 0.0001$ .

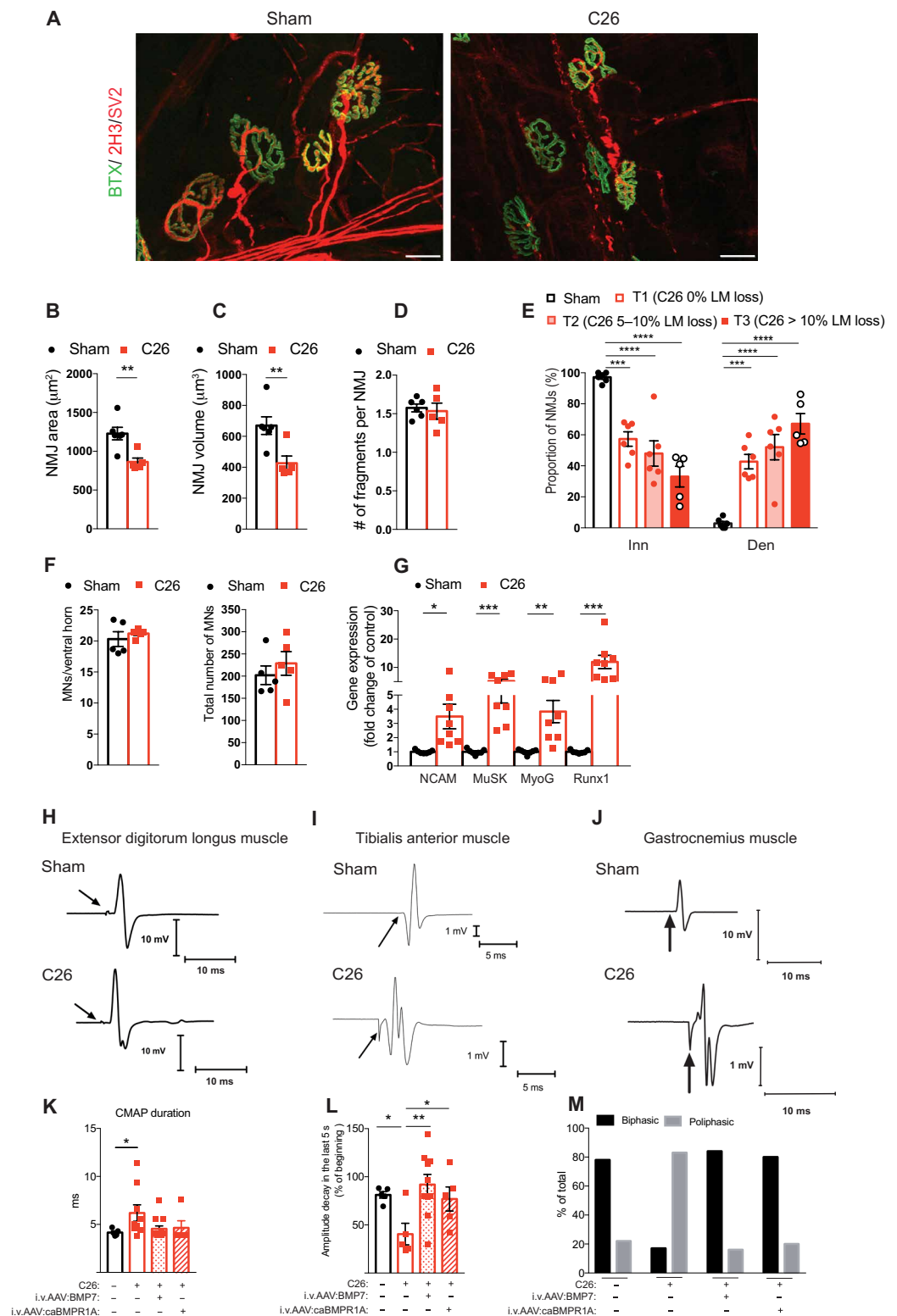
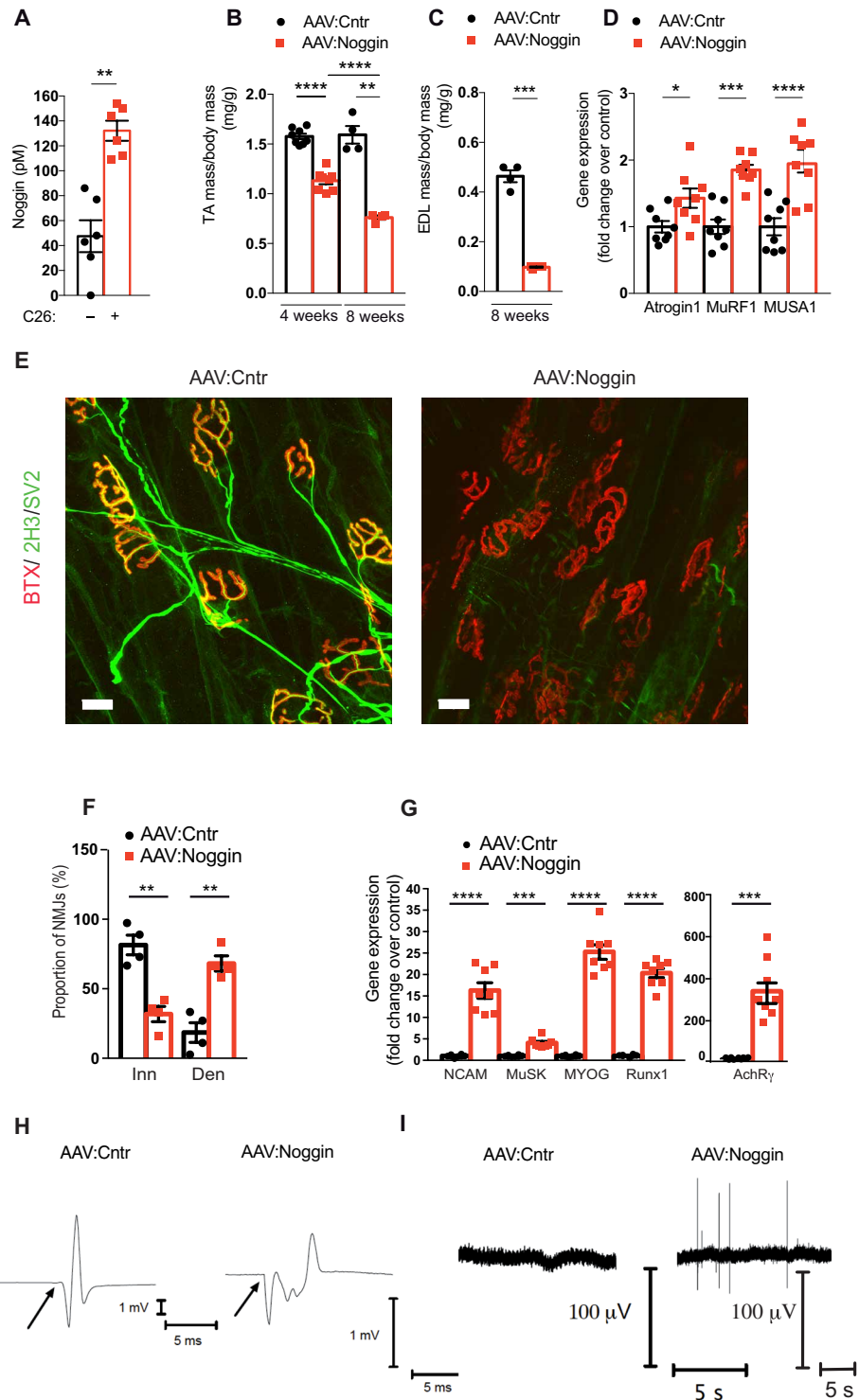


**Fig. 3. Noggin overexpression recapitulates NMJ dismantling and myofiber denervation.**

(A) Noggin protein concentration detected by ELISA in TA muscle lysates of C26 tumor-bearing mice ( $n = 6$ ) compared to sham-injected mice ( $n = 6$ ). (B) Progressive loss of TA muscle mass from C57BL/6 mice examined 4 weeks ( $n = 8$ ) and 8 weeks ( $n = 4$ ) after local administration of AAV:Noggin versus control vector (AAV:Cntr). (C) EDL muscle mass from C57BL/6 mice examined 8 weeks after local administration of AAV:Noggin or control vector (AAV:Cntr) ( $n = 4$ ). (D) Transcription of *Fbxo32* (Atrogin1), *Trim63* (MuRF1), and *Fbxo30* (MUSA1) in TA muscles examined 4 weeks after treatment with AAV:Noggin or AAV:Cntr ( $n = 8$ ). (E) Labeled presynaptic (green) and post-synaptic (red) NMJ components in EDL muscles 8 weeks after injection with AAV:Noggin or AAV:Cntr. Scale bars, 20  $\mu\text{m}$ . (F) Proportion of innervated (Inn) and denervated (Den) NMJs in the EDL muscles depicted in (E) ( $n = 4$ ). (G) Expression of genes associated with denervation in TA muscles 4 weeks after treatment with AAV:Noggin or AAV:Cntr ( $n = 8$ ). (H) Nerve-evoked CMAPs alterations quantified in fig. S11 (F and G) and (I) spontaneous myofiber depolarization revealed by fibrillation potentials in four of five TA muscles treated with AAV:Noggin for 8 weeks (arrows indicate stimulus artifacts) ( $n = 5$ ). Data presented as means  $\pm$  SEM. Paired two-tailed Student's *t* tests were used for experiments comparing two groups (A, C, D, F, and G). One-way ANOVA with Tukey's multiple comparisons test was used to compare the different experimental groups in (B). \* $P < 0.05$ , \*\* $P < 0.01$ , \*\*\* $P < 0.001$ , and \*\*\*\* $P < 0.0001$ .



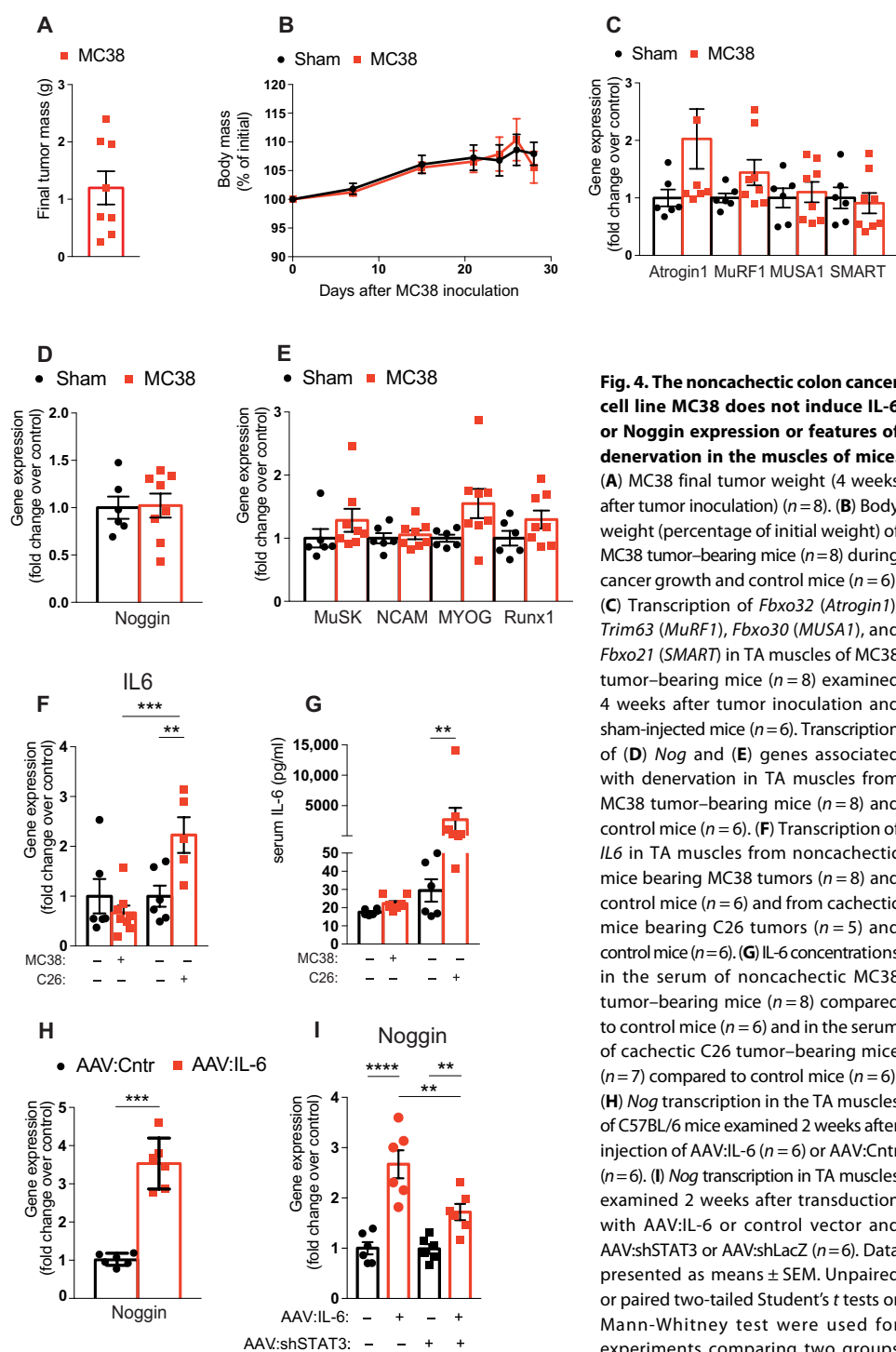
bearing noncachectic MC38 tumors compared to tumor-free mice (Fig. 4, C to E). Because inflammatory cytokines have been identified as mediators of cachexia in the C26 tumor model and because skeletal muscles can constitute a paracrine/autocrine source of inflammatory cytokines such as interleukin-6 (IL-6) (32–34), we measured IL-6 serum concentrations and gene expression in the muscles of mice bearing C26 and MC38 tumors. We found that *IL6* gene expression was increased in the TA muscles of mice bearing cachectic C26 tumors but not in the muscles of mice bearing noncachectic MC38 tumors (Fig. 4F). Concentrations of IL-6 were increased in the sera of C26 tumor-bearing mice but not in MC38 tumor-bearing mice (Fig. 4G). Because Activin A is a negative regulator of muscle mass, which is increased in settings of cachexia associated with tumor growth (26, 27), we measured Activin A in the muscles and sera of MC38 tumor-bearing mice. Although Activin A gene expression did not

change in muscles of mice bearing noncachectic MC38 tumors, the circulating amounts of Activin A were increased in serum of MC38 and C26 mice (fig. S12, C and D) compared to controls. Because IL-6 signatures were elevated in cachectic mice bearing C26 tumors compared with noncachectic mice bearing MC38 tumors, to determine whether IL-6 can promote local Noggin induction, we injected the hindlimb muscles of healthy tumor-free mice with AAV vectors

designed to increase the local expression of IL6. AAV-mediated IL-6 expression in limb muscles for 2 weeks was sufficient to increase the expression of *Nog* (Fig. 4H) and, to a lesser extent, *Chrd*, but not *Grem1* (fig. S12, E and F). Because elevated blood concentrations of IL-6 and Activin A are observed in cachectic mice bearing C26 tumors, we examined the individual and combined effects of these cytokines on *Nog* expression in skeletal muscle. We observed that *Nog* transcription was increased in muscles expressing IL-6 and, to a lesser extent, Activin and further potentiated by the coexpression of the two cytokines (fig. S12G). Cross-reactivity of the pathways was not observed as Activin A expression did not alter phosphorylation of signal transducers and activators of transcription 3 (p-STAT3; fig. S12H) and IL-6 did not affect p-SMAD2 (fig. S12I). These findings are consistent with a synergistic action of the two pathways upon *Noggin* expression in muscles. In contrast to the effects of IL-6 and Activin, overexpression of tumor necrosis factor- $\alpha$ , another proinflammatory cytokine known to signal via IL-6/gp130-independent mechanisms (27, 35), did not promote up-regulation of *Nog* (fig. S12, J to L). These findings support an important role of the IL-6/STAT pathway in *Nog* regulation in skeletal muscle. Consistent with these observations, IL-6 overexpression promoted recruitment of p-STAT3 to several STAT binding sites in the promoter regions of *Nog* and *Chrd* (fig. S13, A and B). Last, by knocking down STAT3 (fig. S13, C and D) in muscles treated with AAV:IL-6, *Nog* expression was blunted when STAT3 was inhibited (Fig. 4I). These data suggest that the IL-6/STAT3 axis contributes to the regulation of *Nog* transcription in muscles.

### Impaired BMP signaling and NMJ remodeling in patients with cachexia-inducing cancer

To establish the clinical significance of our findings of down-regulated BMP pathway activity and NMJ abnormalities early in the manifestation of cancer cachexia in mice, we examined muscle, nerve, and blood parameters for patients diagnosed with cachexia-inducing cancer and cancer-free individuals. Individual enrollment comprised a total of 79 patients admitted for resection of a cancer type commonly associated with cachexia and 23 cancer-free



(B, C, D, E, and H). A one-way ANOVA (F) or a Kruskal-Wallis test (G) with Benjamini, Krieger, and Yekutieli adjustment was performed for experiments comparing more than two groups. A two-way repeated-measures ANOVA with Sidak's multiple comparisons test was performed for experiments comparing multiple variables (I). \*\* $P < 0.01$ , \*\*\* $P < 0.001$ , and \*\*\*\* $P < 0.0001$ .

individuals (Cntr) admitted for abdominal surgery. Patients with cancer were classified on the basis of body mass index (BMI), muscle mass, and body weight loss in the 6 months preceding surgery as either precachectic (PC; weight loss of  $<5\%$ ,  $<2\%$  in individuals with low

muscle mass, or BMI of <20) or as cachectic (C; weight loss of >5%, >2% in individuals with low muscle mass, or BMI of <20). Low muscle mass was defined on the basis of skeletal muscle index (SMI) and BMI in females as an SMI of <38.6 cm<sup>2</sup>/m<sup>2</sup> for a BMI of <30 and an SMI of <46.6 cm<sup>2</sup>/m<sup>2</sup> for a BMI of >30 and in males as an SMI of <52.3 cm<sup>2</sup>/m<sup>2</sup> for a BMI of <30 and an SMI of <54.3 cm<sup>2</sup>/m<sup>2</sup> for a BMI of >30 (36). These criteria identified 39 patients with cancer as PC and 40 patients with cancer as C (fig. S14A). Two percent of all patients approached for study enrollment declined participation. The three groups (Cntr, PC, and C) were comparable for parameters of sex, age, comorbidities, and medications, whereas the C group, as expected, presented a substantially reduced BMI and increased recent weight loss (table S1). Characteristics for the oncology patients and the indication for which the control individuals had surgery are reported in tables S2 and S3, respectively. Analysis of gene expression was performed for abdominal muscle biopsies from all 102 patients, as planned. When compared to Cntr, *NOG* gene expression was up-regulated in muscle biopsies from PC and C patients with cancer (Fig. 5A). In addition to increased expression of *NOG*, expression of the E3 ligases *FBXO30* (*MUSA1*) and *TRIM63* (*MuRF1*) were also increased in the muscle biopsies of PC and C patients with cancer (Fig. 5B and fig. S14B), whereas *FBXO32* (*Atrogin1*) and *FBXO21* (*SMART*) were not increased (fig. S14B-D).

Because ligands that promote SMAD2/3 signaling constitute another mode by which the actions of endogenous BMPs may be antagonized, we analyzed serum concentrations of Activin A and the transcription of Activin A in muscle biopsies from patients. The Activin A enzyme-linked immunosorbent assay (ELISA) assay was performed using only nonhemolyzed (nh) samples from a subset of 65 patients with cachexia-inducing cancer (PC, *n* = 32; C, *n* = 33) and 15 cntr (fig. S14A). The three subgroups (Cntr<sub>nh</sub>, PC<sub>nh</sub>, and C<sub>nh</sub>) were comparable for parameters of sex, age, and medications, whereas the C<sub>nh</sub> group presented a reduced BMI, an increased magnitude of recent weight loss, and increased incidence of comorbidities, as reported in table S4. Characteristics for this subset of oncology patients and the indication for which the cntr individuals had surgery are depicted in tables S5 and S6, respectively. The serum concentration of Activin A was increased for C<sub>nh</sub> patients (fig. S14E) in agreement with previous reports (12, 13), and the transcription of Activin A was not different in the muscle biopsies of patients with cancer (fig. S14F).

Because cancer growth results in an alteration of NMJ before cachexia onset in rodents, we subsequently examined the plasma concentrations of biomarkers of NMJ remodeling and degeneration in patients. During NMJ degeneration, a cleaved form of Agrin, a key protein component of the terminal presynaptic structure required for NMJ stability, is released into the circulation (37–39). We observed that the concentration of soluble C-terminal Agrin fragment was increased in the plasma of PC<sub>nh</sub> and C<sub>nh</sub> patients with cancer when compared to Cntr<sub>nh</sub> (Fig. 5C). Measurement of soluble NCAM, another circulating marker of synapse degeneration (40, 41), identified a similar effect of increased concentration in the serum samples of PC<sub>nh</sub> and C<sub>nh</sub> patients with cancer when compared to Cntr<sub>nh</sub> (Fig. 5D).

To assess whether morphological markers presented evidence of muscle and nerve pathology, we examined sections of muscle biopsies from patients. Analyses were conducted using only samples free of technical limitations (ftl); (criteria for exclusion included swollen/damaged

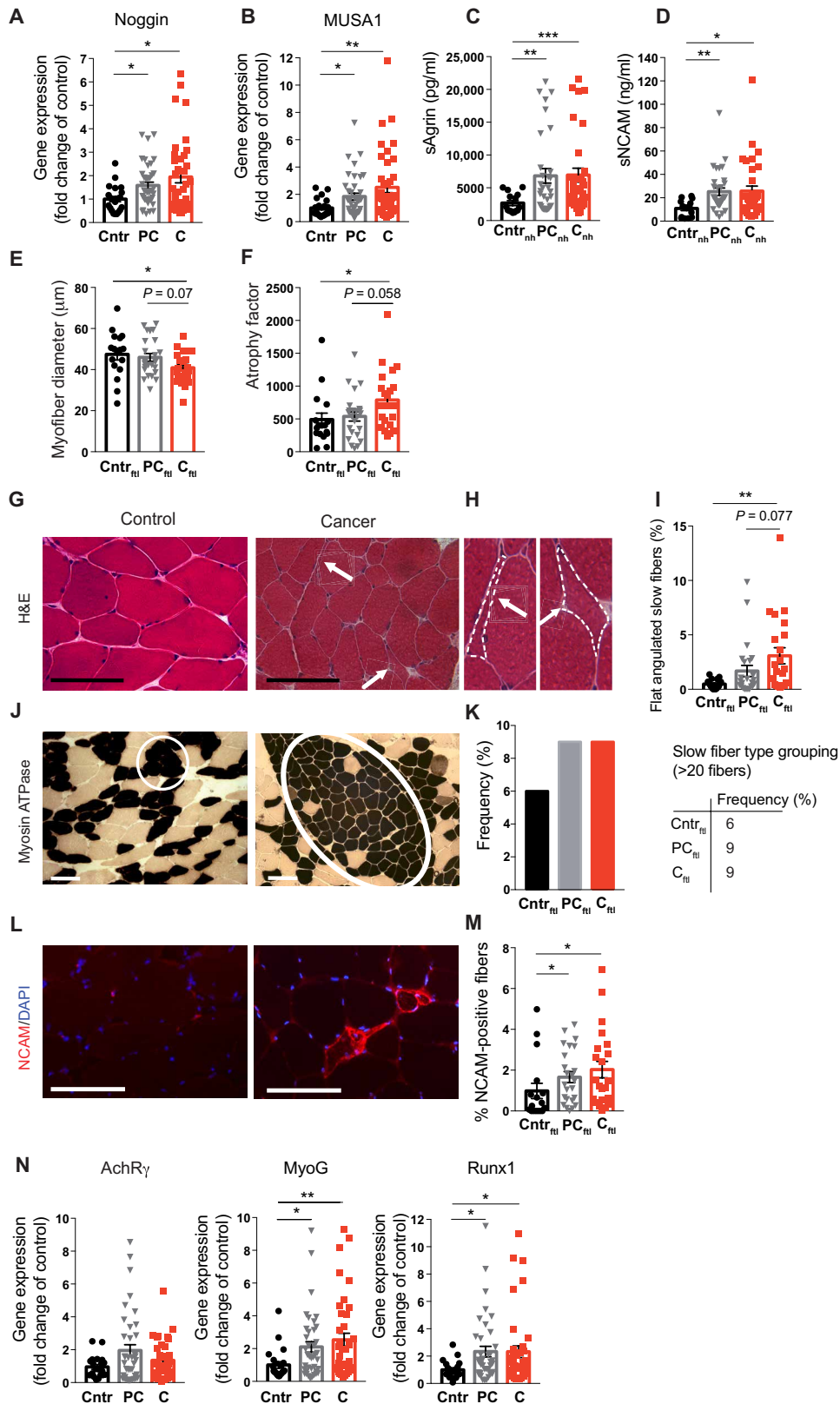
fibers consequent to imperfect freezing procedure, incorrect muscle fiber orientation in the plane of section, staining artifacts, and insufficient biopsy quantity) from a subset of 46 patients with cachexia-inducing cancer (PC, *n* = 24; C, *n* = 22) and 17 Cntr (fig. S14A). The three subgroups (Cntr<sub>ftl</sub>, PC<sub>ftl</sub>, and C<sub>ftl</sub>) were comparable for parameters of sex, age, comorbidities, and medications, whereas the C<sub>ftl</sub> group presented with increased recent weight loss (table S7). Tumor type, the stage of cancer, and the disease for which control patients had surgery are reported in tables S8 and S9. Morphological analyses of muscle biopsies revealed the presence of severely atrophic fibers in C<sub>ftl</sub> patients with cancer compared to Cntr<sub>ftl</sub> patients (Fig. 5, E to H). Analysis of muscle biopsy cryosections identified a decrease in myofiber diameter in C<sub>ftl</sub> when compared to Cntr<sub>ftl</sub> (Fig. 5E). In line with previous observations related to sexual dimorphism (42), biopsies of female Cntr<sub>ftl</sub> and PC<sub>ftl</sub> patients comprised muscle fibers of reduced diameter compared to males. (fig. S14G). The atrophy factor, an index of extremely small muscle fibers (43), was increased only in C<sub>ftl</sub> patients (Fig. 5F). Severely atrophic fibers exhibited features characteristic of denervation such as reduced circularity and increased angularity (Fig. 5, G to I). Moreover, histochemical reaction of sections from muscle biopsies for slow and fast myofibrillar adenosine triphosphatase (ATPase) activity revealed extensive grouping of muscle fiber types in patients with cancer (Fig. 5, J and K, and fig. S14H). This phenotype is consistent with fiber type grouping observed in other settings where previously denervated muscle fibers have reacquired innervation from a motor nerve supplying a neighboring muscle fiber and subsequently adopted the myosin ATPase profile of the adjacent motor unit (44, 45). Large groupings (>20 fibers) of slow type fibers were more common in the muscle biopsies of C<sub>ftl</sub> patients than Cntr<sub>ftl</sub> and more commonly observed in the muscles of PC<sub>ftl</sub> patients (Fig. 5K). Consistent with a denervation phenotype, the prevalence of NCAM-positive muscle fibers was also increased in the muscles of PC<sub>ftl</sub> and C<sub>ftl</sub> patients with cancer compared to Cntr<sub>ftl</sub> (Fig. 5, L and M). Similarly, indicators of NMJ remodeling and degeneration observed in serum samples and further supported by morphological analyses of muscle biopsies of patients with cancer were associated with increased transcription of genes associated with NMJ remodeling, including *MYOG* and *RUNX1* but not *CHRNG*, in the biopsies of PC and C patients compared with Cntr (Fig. 5N). Collectively, these findings reported for patients with cancer are consistent with the aforementioned animal data that describe the remodeling and degeneration of the NMJ in advance of advanced cachexia, which is associated with impaired BMP-SMAD1/5/8 signaling.

### Tilorone administration restores BMP-mediated signaling, ameliorates muscle wasting, and prolongs survival in tumor-bearing mice

Having identified that BMP-SMAD1/5/8 signaling is suppressed in the muscles of cachectic mice and that restoring its activity via genetic interventions is beneficial in the setting of cachexia, we investigated whether pharmacological interventions capable of sustaining or enhancing BMP signaling could also protect from cachexia. Previously, an *in vitro* chemical compound screen identified tilorone, which has been used clinically as an antiviral and anti-inflammatory medication, as capable of increasing *Bmp7* expression and BMP-mediated signaling in cultured human lung epithelial cells and mouse models of pulmonary fibrosis (46). We investigated the effects of repeated tilorone administration upon the progression

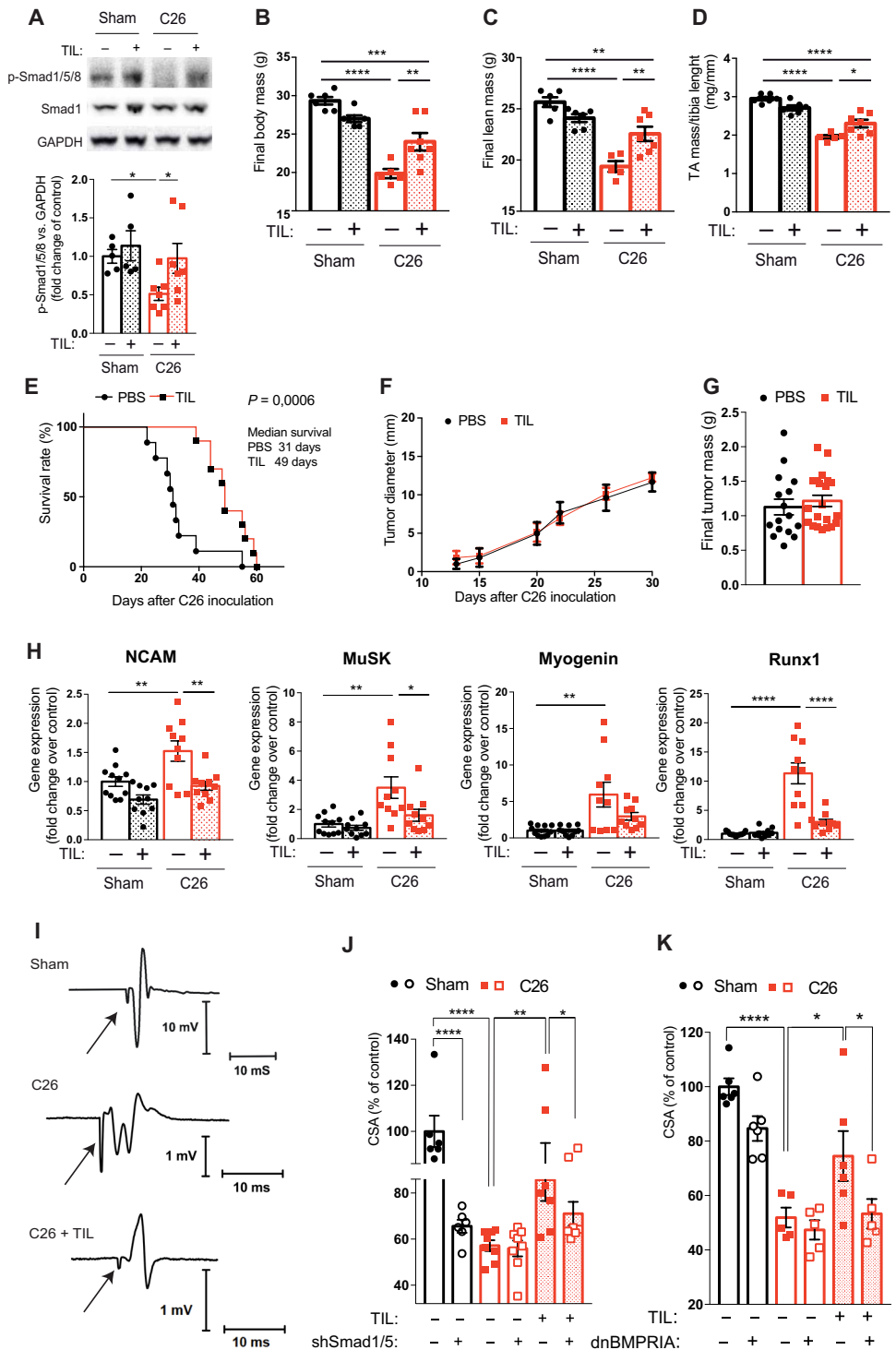
**Fig. 5. BMP pathway impairment and NMJ remodeling in the muscles of patients bearing cachexia-inducing cancers.**

(A) *NOG* (Noggin) and (B) *FBXO30* (*MUSA1*) gene expression analysis in the rectus abdominis muscles of precachectic (PC) and cachectic (C) patients with cancer compared to (Cntr) healthy individuals (Cntr,  $n=23$ ; PC,  $n=39$ ; C,  $n=40$ ). Circulating concentrations of (C) soluble Agrin in the plasma and of (D) soluble NCAM in the serum of nonhemolyzed (nh) samples from Cntr<sub>nh</sub> ( $n=15$ ), PC<sub>nh</sub> ( $n=32$ ), and C<sub>nh</sub> ( $n=33$ ) patients. (E) Mean diameter and (F) Atrophy factor in rectus abdominis muscle fibers from free of technical limitations (ftl) Cntr<sub>ftl</sub> ( $n=17$ ), PC<sub>ftl</sub> ( $n=24$ ), and C<sub>ftl</sub> ( $n=22$ ) patients. (G) Representative hematoxylin and eosin (H&E)-stained cryo-sections of rectus abdominis muscle biopsies from a cachectic patient with cancer identifying the presence of flat shaped, angulated, and severely atrophic muscle fibers (arrows) compared to a healthy individual. Scale bars, 100  $\mu$ m. (H) Higher magnification images of the muscle fibers indicated by the arrows in (G). Arrows and dashed lines indicate myofibers of angular/flat shape, typical of denervation. (I) Proportion of flat-shaped, angulated slow fibers in Cntr<sub>ftl</sub> ( $n=17$ ), PC<sub>ftl</sub> ( $n=24$ ), and C<sub>ftl</sub> ( $n=22$ ) patients. (J) Histochemical reaction of cryosections for myosin ATPase isoforms identifies slow fiber type grouping (dark staining) in a muscle biopsy from a cachectic patient with cancer compared to an age-matched control. Fiber-type grouping (highlighted by white circles) was identified on the basis that at least one muscle fiber was completely surrounded by fibers of the same type. Scale bars, 100  $\mu$ m. (K) Frequency histogram of very large (>20 fibers) slow fiber type grouping in Cntr<sub>ftl</sub> ( $n=17$ ), PC<sub>ftl</sub> ( $n=24$ ), and C<sub>ftl</sub> ( $n=22$ ) patients. For each group, the frequency values expressed in percentage are reported in the table on the right. (L) Immunolabeling of NCAM (red) identifying NCAM-positive denervated fibers in a rectus abdominis muscle biopsy from a cachectic patient with cancer. Scale bars, 100  $\mu$ m. (M) Proportion of NCAM-positive muscle fibers in rectus abdominis biopsies from Cntr<sub>ftl</sub> ( $n=17$ ), PC<sub>ftl</sub> ( $n=24$ ), and C<sub>ftl</sub> ( $n=22$ ) patients. (N) *CHRNA3* AchR $\gamma$ , *MYOG*, and *RUNX1* gene expression in the rectus abdominis muscles of PC ( $n=39$ ) and C ( $n=40$ ) patients with cancer compared to healthy individuals (Cntr) ( $n=23$ ). Data presented as means  $\pm$  SEM. One-way ANOVA (E) or Kruskal-Wallis test (A, B, C, D, F, I, M, and N) with adjustment for multiple testing (Benjamini, Krieger, and Yekutieli). \* $P < 0.05$ , \*\* $P < 0.01$  and \*\*\* $P < 0.001$ .



Downloaded from <https://www.science.org> at University of Pennsylvania on January 30, 2023

**Fig. 6. Tilorone treatment reactivates the BMP-SMAD1/5/8 pathway in the muscles of tumor-bearing mice, prevents muscle wasting, and prolongs survival without affecting tumor size.** (A) Immunoblot and densitometric analysis of p-SMAD1/5/8 in the TA muscles of C26 tumor-bearing mice treated with tilorone ( $n = 7$ ) or vehicle ( $n = 7$ ), and control mice ( $n = 5$ ). (B) Body mass, (C) lean mass, and (D) TA muscle mass of C26 tumor-bearing mice treated with vehicle or tilorone, and control mice [control mice phosphate-buffered saline (PBS)-treated,  $n = 6$ ; control mice tumor-infiltrating lymphocyte (TIL)-treated,  $n = 6$ ; C26 mice PBS-treated,  $n = 5$ ; C26 mice TIL-treated,  $n = 7$ ]. (E) Survival rate of C26 tumor-bearing mice administered vehicle ( $n = 9$ ) or tilorone ( $n = 10$ ). (F) Tumor growth progression ( $n = 7$  per group) and (G) tumor mass at experimental end point in C26 tumor-bearing mice treated with vehicle ( $n = 16$ ) or tilorone ( $n = 21$ ). (H) Transcription of genes associated with denervation in GAS muscles from C26 tumor-bearing mice and sham-injected mice, treated with vehicle or tilorone (control mice PBS-treated,  $n = 11$ ; control mice TIL-treated,  $n = 10$ ; C26 mice PBS-treated,  $n = 10$ ; C26 mice TIL-treated,  $n = 10$ ). (I) Representative electromyographic traces of nerve-evoked CMAPs recorded from the TA muscles of sham and C26 tumor-bearing mice receiving vehicle or tilorone treatment. Arrows indicate stimulus artifacts.  $n = 5$  animals per group. Quantification reported in fig. S15 (D and E). (J) Cross-sectional area of GFP-positive TA muscle fibers from C26 tumor-bearing mice treated with vehicle ( $n = 8$ ) or tilorone ( $n = 7$ ) and transfected by electroporation with bicistronic expression plasmids encoding eGFP, and shRNAs against SMAD1 and SMAD5 or scrambled shRNA, and from control mice ( $n = 6$ ). (K) Cross-sectional area of GFP-positive TA muscle fibers transfected by electroporation with constructs expressing eGFP or eGFP and dnBMPRI1A, obtained from C26 tumor-bearing mice treated with vehicle ( $n = 5$ ) or tilorone (with eGFP,  $n = 6$ ; with dnBMPRI1A,  $n = 5$ ) or from control mice ( $n = 6$ ). Data presented as means  $\pm$  SEM. Unpaired two-tailed Student's  $t$  tests or Mann-Whitney test were used for experiments comparing two groups (F and G). A two-way ANOVA with Benjamini, Krieger, and Yekutieli adjustment (A) or with Sidak's multiple comparisons test (B, C, D, H, and K) or a two-way repeated-measures ANOVA with Sidak's multiple comparisons test (J) was performed for experiments comparing multiple variables. Gehan-Breslow-Wilcoxon test was used to compare survival curves (E). \* $P < 0.05$ , \*\* $P < 0.01$ , \*\*\* $P < 0.001$ , and \*\*\*\* $P < 0.0001$ .



of cancer cachexia in mice bearing C26 tumors. p-SMAD1/5/8 was reduced in the limb muscles of tumor-bearing mice receiving vehicle and was restored to normal values in mice treated with tilorone (Fig. 6A). To further dissect the connection between tilorone and

SMADs, we overexpressed SMAD6, an intracellular negative regulator of type I BMP receptor-SMAD1/5/8 signaling. SMAD6 expression blunted the beneficial effects of tilorone on p-SMAD1/5/8 in the muscles of C26 tumor-bearing mice (fig. S15A). Consistent with

these findings, AAV-mediated SMAD6 overexpression prevented tilorone-mediated nuclear localization of p-SMAD1/5/8 in cachectic muscles (fig. S15A). Although tilorone administration did not completely protect against cachexia, mice treated with tilorone demonstrated a conservation of body mass that was associated with the preservation of lean mass and muscle mass (Fig. 6, B to D, and fig. S15B) concomitant with diminished expression of key atrophy-related genes (fig. S15C). Furthermore, survival studies demonstrated that C26 tumor-bearing mice administered tilorone survived on average 58% longer than tumor-bearing mice receiving vehicle (Fig. 6E). Tumor mass and diameter did not differ between cohorts receiving tilorone or vehicle over the study duration or in cohorts measured at study end points, indicating that the observed results were not a consequence of treatment effects upon tumor growth (Fig. 6, F and G). Compared with the muscles of tumor-bearing mice receiving vehicle, the muscles of tumor-bearing mice administered tilorone exhibited reduced expression of *Fbxo32* (Atrogin1), *Trim63* (MuRF1), and *Fbxo30* (MUSA1) and denervation markers *Ncam1*, *Musk*, *Myog*, and *Runx1* (Fig. 6H and fig. S15C). In addition, tilorone treatment preserved CMAP parameters in the hindlimb muscles of tumor-bearing mice, providing an electromyographic measure consistent with maintenance of functional NMJs (Fig. 6I and fig. S15, D and E).

To test whether the beneficial effect of tilorone is dependent on stimulation of the BMP-SMAD1/5/8 pathway, we examined the effects of blocking the BMP pathway at different levels in the muscles of tumor-bearing mice receiving tilorone. First, we used previously validated short hairpin RNA (shRNA) constructs targeting SMAD1 and SMAD5 (17). These constructs efficiently knocked down *Smad1/5* transcripts (fig. S17F) and abolished SMAD1/5 activation of the *Id1* reporter (a readout of BMP-SMAD1/5/8 signaling) in muscles (fig. S15G). Inhibition of SMAD1/5 induced muscle wasting in tumor-free mice but did not exacerbate muscle loss in C26 tumor-bearing mice (Fig. 6J). Knockdown of SMAD1/5 inhibited the protective effects of tilorone upon muscle fiber size in cachectic mice (Fig. 6J). Second, we cloned a dominant-negative catalytically inactive form of BMPRI1A (dnBMPRI1A). The dnBMPRI1A construct was functionally validated for its capability to inhibit the transcription of a reporter of SMAD1/5 activity (fig. S15H). Overexpression of dnBMPRI1A blocked the protective effects of tilorone upon muscle fiber size in cachectic mice (Fig. 6K). Third, we blocked the BMP pathway by overexpressing Noggin. AAV-mediated Noggin overexpression decreased muscle fiber size in control mice but did not exacerbate muscle atrophy in C26 tumor-bearing mice. In contrast, overexpression of Noggin blunted the protective effect of tilorone treatment upon muscle fiber size in cachectic mice (fig. S15I). Thus, the findings demonstrate that drug-based interventions that are capable of enhancing BMP-SMAD1/5/8 signaling can confer benefits upon skeletal muscles and the NMJ in a model of cancer cachexia.

## DISCUSSION

Up to 80% of patients with cancer present evidence of weight loss consistent with the onset/progression of catabolic processes contributing to cachexia (3). Confirmation of cachexia according to clinical guidelines is an independent prognostic factor that lowers patients' responses to chemo- and radiotherapy and has been directly attributed to death in up to 30% of patients with advanced cancer (3). Muscle wasting and fatigue are the primary feature of cachexia and preventing muscle loss has been demonstrated to prolong survival in mouse models

of cancer cachexia independent of effects on tumor growth and white adipose tissue loss (5). Thus, the development of therapies to preserve and/or restore muscle mass and functionality could potentially enhance patients' quality of life, response to therapies, and life span.

BMP signaling through SMAD1/5/8 was recently identified as an important regulator of muscle homeostasis (17, 18). The BMP-SMAD1/5/8 axis negatively regulates the E3 ubiquitin ligase *Fbxo30* (Musa1) required for neurogenic muscle atrophy (17, 18). Experimental inhibition of BMP signaling during catabolic conditions such as prolonged fasting or denervation derepresses *Fbxo30* (Musa1) transcription, resulting in excessive muscle wasting and weakness phenocopying cachexia (17, 18). In the present studies, we found that p-SMAD1/5/8, a readout of BMP-mediated signaling, was strongly decreased in skeletal muscles from different models of cancer cachexia. Down-regulation of BMP signaling occurs early in the onset of muscle wasting and remains diminished as muscle wasting becomes more severe with cancer progression. In line with the down-regulation of BMP signaling, we observed that *Fbxo30* (Musa1) gene expression was increased in the muscles of cachectic mice. Together, these observations support the concept that inhibited BMP-SMAD1/5/8 signaling derepresses catabolic processes in muscles that are associated with the progression of cachexia. Moreover, transcription of *Nog*, an extracellular inhibitor of BMPs, was increased in the muscles of cachectic mice, presenting a mechanism by which BMP-SMAD1/5/8 signaling is inhibited in settings of advanced cancer, with deleterious consequences.

Supporting the hypothesis that the suppression of BMP-SMAD1/5/8 signaling contributes to the loss of muscle mass associated with cachexia, reactivation of BMP-dependent signaling by a caBMPRI1A was sufficient to prevent tumor-induced muscle atrophy. Knocking down *Fbxo30* (MUSA1) also prevented muscle loss in tumor-bearing mice, demonstrating that this E3 ubiquitin ligase, which is a bona fide target of SMAD1/5/8, is required to promote muscle atrophy associated with cachexia. Increasing BMP7 expression in muscles via gene delivery was able to reproduce some of the protective effects mediated by caBMPRI1A expression or *Fbxo30* (MUSA1) knockdown, thereby demonstrating that a muscle-directed BMP-based intervention may have therapeutic potential. Furthermore, the administration of tilorone to mice bearing cachexia-inducing C26 tumors pharmacologically reactivated BMP signaling in skeletal muscle and was associated with reduced loss of lean mass and a marked extension of life span without affecting tumor growth. Loss of body mass in mice bearing cachexia-inducing C26 tumors and *Inha*<sup>-/-</sup> mice is associated with high circulating concentrations of Activin A and inflammatory cytokines such as IL-6 (26, 27). In addition, increased local concentrations of Activin A are sufficient to induce loss of lean mass in the absence of tumors, which is primarily an effect of muscle wasting (14, 27). We observed that the activity of the BMP-SMAD1/5/8 pathway is also blunted in muscles overexpressing Activin A and that reactivation of BMP-SMAD1/5/8 signaling by caBMPRI1A or BMP7 is able to attenuate Activin A-mediated muscle atrophy. These findings are consistent with reports of Activin A acting as a competitive inhibitor of lower affinity BMP ligands that can engage type II receptors, such as BMP7 (47), and highlight the importance of considering the potential impact of Activin A and related ligands upon BMP-Smad1/5/8 signaling in muscle.

The most unexpected finding was the observed loss of NMJ integrity and the presence of denervated muscle fibers in tumor-bearing mice in advance of muscle atrophy. The combination of low-amplitude

short-duration myopathic motor unit potentials, neurogenic polyphasic potentials, and prolonged duration is consistent with a denervation process at the endplate region together with marked reinnervation. Mechanistically, we identified BMP signaling as critical for mediating NMJ plasticity in the setting of cachexia in mice. The BMP pathway is known to regulate peripheral synaptic development and plasticity in *Drosophila* (19–21), but its role in controlling postnatal NMJ remodeling in adult mammals, particularly in pathological contexts, remains to be elucidated. Our studies identify that a functional impairment of the NMJ associated with diminished BMP-SMAD1/5/8 signaling is prevalent in the muscles of cachectic tumor-bearing mice.

Our findings demonstrate that disruption of the NMJ in cancer cachexia occurs via the deterioration of presynaptic architecture and that this phenotype is recapitulated by experimentally increasing Noggin expression in the muscles of healthy mice. We observed *Nog* up-regulation and denervation in experimental settings of tumor growth where cachexia develops and the expression of *IL6* in muscles is increased. Analyses of mice bearing noncachectic tumors and of IL-6 and Activin A effects in the muscles of tumor-free mice support a synergistic role for these cytokines in inducing *Nog* expression and muscle wasting. Because Noggin overexpression is sufficient to cause NMJ impairment and neurogenic muscle atrophy (including the up-regulation of genes associated with denervation and NMJ remodeling), we propose that endogenous BMP ligands play an important role in the maintenance of the adult mammalian NMJ. Because increasing BMP signaling via BMP7 gene delivery or treatment with tilorone is able to correct measures of NMJ function and attenuate muscle atrophy in mice bearing cachexia-inducing tumors, we contend that interventions that promote the activity of specific BMP ligands or downstream signaling in muscles and motor nerves have potential utility in the prevention and treatment of muscle wasting and dysfunction underlying cancer cachexia.

To corroborate whether our findings of NMJ abnormalities associated with up-regulation of *Nog* and *Fbxo30* (MUSA1) in the muscles of cachectic mice were also observed in humans, we analyzed muscle biopsies of patients diagnosed with cachexia-inducing cancers and cancer-free individuals, as a single time-point cross-sectional study. Having stratified patients with cancer into precachectic and cachectic subgroups and verified that they and the cancer-free cohort were homogeneous for potential confounding factors, we observed that *NOG* and *FBXO30* (MUSA1) expression was increased in the muscles of precachectic and cachectic patients compared to cancer-free individuals, suggesting a precocious down-regulation of the BMP pathway, as observed in mice. In addition, consistent with our preclinical findings of NMJ impairment in tumor-bearing mice, NMJ instability, as indicated by an increased incidence of NCAM-positive muscle fibers, clustering of muscle fibers by type, and transcription of denervation markers, was observed in the biopsies of patients with cancer before the onset of cachexia. Concomitantly, patients with cancer presented with increased concentrations of soluble NCAM and Agrin fragment, as circulating markers of NMJ degeneration. These indicators of NMJ disruption and remodeling in patients with cancer offer a potential explanation for earlier reports of a “carcinomatous neuromyopathy” defined by electrophysiological characteristics that include atypical motor unit potentials displaying a notable mixture between myopathic and neurogenic potentials (48, 49).

It is important to note that we observed increased expression of *NOG* and *FBXO30* (MUSA1) and increased blood concentrations of

soluble Agrin and NCAM in PC patients. These findings demonstrate that impaired BMP signaling in muscle and NMJ degeneration/remodeling is not merely a consequence of cachexia but potentially contributes to disease progression, as we have observed in mice. These clinical observations suggest that monitoring Noggin, MUSA, and denervation markers could offer potential indicators of increased risk of muscle wasting and functional decline in patients with cancer who are not yet cachectic. An additional consideration is that despite observing increased expression of Noggin in the muscles of cachectic mice and patients with cancer, it cannot be excluded that nonmuscle tissues and tumors may also be a source of Noggin. For instance, increased tumor expression of Noggin has been associated with reduced survival in patients with pancreatic and colorectal carcinoma, two of the most common populations to suffer severe cachexia (50–52). Consideration of those clinical data and our findings reported herein support further examination of the biological role of Noggin as a potential disease indicator and therapeutic target. Interactions between the tumor and host may potentially drive other mechanisms that can also impair BMP-Smad1/5/8 signaling. Ligands that can antagonize receptor engagement by BMP proteins or alter the sensitivity of the BMP-Smad1/5/8 axis in muscle fibers and motor nerves can arise from endocrine, paracrine, or autocrine mechanisms and differ between individuals due to their genetic/epigenetic attributes. Such variability between individuals reiterates that the molecular etiology of cancer cachexia is multifactorial and diverse, even among patients with a similar tumor type. Biological diversity as a determinant of tumor malignancy and patient response remains one of the greatest challenges facing the development of better diagnostics and interventions for cancer. Hence, further study of mechanisms that contribute to regulation of BMP signaling and its effect on motor nerve and muscle function may help to deconvolute the molecular etiology of cachexia.

A limitation of our studies concerns the challenges encountered in studying the kinetics of cachexia onset in mouse models versus patients. Most existing mouse models of cancer cachexia progress more quickly than what is observed in the clinical setting, which may have consequences for the study of certain events such as cycles of NMJ remodeling. In addition, although we have observed similar findings between mouse limb/abdominal muscles and human abdominal muscle biopsies, our inability to sample the entirety of specific trunk and limb muscles in patients may underestimate the full extent to which denervation may occur in individual patients’ muscles. The genetic diversity of humans, as well as human cancers, also contributes to variability in the extent to which biological processes promote the development of cachexia in individuals. We have focused our research on patients with pancreatic and colon cancer due to the high prevalence of cachexia in these individuals. Whether other types of cancer promote NMJ instability remains to be explored. Because new mouse models of cachexia-inducing cancers continue to be developed (53), future studies combining preclinical and patient analyses will help to determine to what extent perturbed BMP signaling and NMJ impairment are features of cachexia associated with cancers of different origins.

Our cross-sectional study design did not enable us to unequivocally demonstrate a causal link between reduced BMP signaling, NMJ remodeling, and the development of cancer cachexia in patients. Although confirming true causality would require the longitudinal study of patients with concurrent examination of the effects of molecular loss/rescue of function to confirm a mechanism of action,

the impact of such studies on patients is hard to justify, without prior observational findings allied with a mechanistic basis established in animal models. For ethical reasons, the patients enrolled in this study did not complete multiple computed tomography scans and contribute multiple biopsies over a time course, thereby preventing our examination of temporal processes related to BMP signaling, NMJ pathology, and cachexia. Notwithstanding these constraints, our clinical observations are important because they demonstrate that perturbed BMP signaling and associated NMJ pathology are evident in patients with pancreatic and colon cancer, for whom cachexia is often a critical feature of disease progression. Moreover, our observations establish that impaired BMP signaling and NMJ remodeling can be detected in patients not yet characterized as cachectic, consistent with our preclinical observations of mouse models. The findings demonstrate that impaired BMP signaling and NMJ pathology are not simply the consequence of advanced cachexia nor can they be excluded as a contributing factor in the manifestation of muscle atrophy and weakness in cachexia. We propose that further consideration of these disease features could have important implications for understanding why specific individuals experience debilitating loss of muscle function and may help to inform personalized treatment plans and individual inclusion in prospective trials of experimental interventions.

Collectively, the results presented identify perturbed BMP-SMAD1/5/8 signaling and disruption of the NMJ as important features in relation to debilitating muscle wasting and dysfunction associated with cancer. Markers of BMP signaling and NMJ pathology may provide valuable readouts to monitor processes contributing to cachexia and the efficacy of prospective interventions. A corollary to the findings is that interventions that aim to treat cachexia by up-regulating protein synthesis or inhibiting protein breakdown in muscles may offer limited functional benefit if NMJ architecture and functionality remain compromised. Another consideration is that the potential for NMJ impairment arising may revise the indications for some anticancer agents with known risks of lean mass loss and neurotoxic effects. The findings described here identify the BMP-SMAD1/5/8 pathway as a promising target for consideration in the development of personalized diagnostics and therapeutics to preserve/restore muscle and motor nerve attributes that maintain physical and metabolic functionality and counter the impact of cancer cachexia. Future studies are recommended to consider the relevance of these findings to other cancer types where cachexia is also observed.

## MATERIALS AND METHODS

### Study design

The objective of this study was to understand the role of the BMP pathway in regulating the mass and innervation status of skeletal muscle in tumor-bearing laboratory mice and patients with cancer. Controlled laboratory experiments were conducted in mice to examine the time course and mechanisms of action associated with disease progression, and a single time-point cross-sectional study was undertaken in patients with cancer or healthy control patients. Experimental interventions for gain or loss of function in mice included the use of AAV vectors, the plasmid-mediated expression by electroporation, and the administration of pharmacological agents. A variety of analyses were conducted in skeletal muscle samples of mice and patients including gene and protein expression using real-time PCR and Western blotting, respectively, morphological

analyses conducted using microscopy and physiological function using electromyography and circulating quantities of protein by ELISA assay. Sample sizes were calculated using size power analysis methods for a prior determination, on the basis of the SD and effect size previously obtained using the experimental methods used in the study. With a type I error of 0.05 and a power of 0.80, we calculated the minimal sample size for each group to be at least four mice. Considering a likely drop-off effect of 10%, we set sample size for each group to five mice. To reduce the SD, we minimized physiological variation using mice of the same sex and same age. Final end points were determined prospectively and were based on the degree of cachexia (~25% loss of initial body mass). Exclusion criteria for animals were applied in case of death, cannibalism, and the presence of severe clinical alteration of vital physiological functions and ulceration induced by the tumor mass. Exclusion criteria for samples were applied in case of histological artifacts (freeze- and cut-damaged tissues), RNA and protein degradation, and blood hemolysis. We included mice from different breeding cages by random allocation to the different experimental groups. Mouse experiments were not performed with blinding; however, when possible (real-time PCR, Western blot, NMJ and muscle morphology evaluation, and ELISA assays), experimenters were blinded to the nature of the samples using number codes until final data analysis was performed.

To establish whether our findings in the muscles of cachectic mice were relevant to cachexia in humans, we analyzed muscle biopsies and blood samples of patients diagnosed with cachexia-inducing cancers, stratified into C and PC subgroups as defined by Fearon *et al.* (1), compared to patients undergoing surgery for nonneoplastic noninflammatory diseases (Cntr). Inclusion criteria were individuals >18 years who gave freely written informed consent. Exclusion criteria were presence of active inflammatory or infective diseases, known myopathies, or viral infections (such as hepatitis c virus, hepatitis B virus, and HIV). Control patients were excluded if having history of cancer.

### Statistical analysis

Statistical tests (Student's *t* test or Mann-Whitney test, one-way analysis of variance (ANOVA) or Kruskal-Wallis test, two-way ANOVA, and the multiple testing procedures) were used as described in the figure legends and were conducted upon verification of the normality assumption using the Kolmogorov-Smirnov test (where applicable). For all graphs, data are presented as means  $\pm$  SEM. Differences between groups were considered statistically significant when the *P* value obtained was less than 0.05; the *P* values are reported in the figure legends. All the *n* reported in the figure legends are referred to biological replicates. Every experiment was replicated at least twice. Animal cohorts were repeated to establish confidence in the reproducibility of data presented. Initial optimization of experimental reagents such as dose-response experiments was performed. Statistical analyses were performed using GraphPad Prism 7.0a (GraphPad).

## SUPPLEMENTARY MATERIALS

[stm.sciencemag.org/cgi/content/full/13/605/eaay9592/DC1](https://stm.sciencemag.org/cgi/content/full/13/605/eaay9592/DC1)

Supplementary Methods

Figs. S1 to S15

Tables S1 to S10

Data file S1

References (54–92)

[View/request a protocol for this paper from Bio-protocol.](#)

## REFERENCES AND NOTES

- K. Fearon, F. Strasser, S. D. Anker, I. Bosaeus, E. Bruera, R. L. Fainsinger, A. Jatoi, C. Loprinzi, N. MacDonald, G. Mantovani, M. Davis, M. Muscaritoli, F. Ottery, L. Radbruch, P. Ravasco, D. Walsh, A. Wilcock, S. Kaasa, V. E. Baracos, Definition and classification of cancer cachexia: An international consensus. *Lancet Oncol.* **12**, 489–495 (2011).
- M. Muscaritoli, S. D. Anker, J. Argiles, Z. Aversa, J. M. Bauer, G. Biolo, Y. Boirie, I. Bosaeus, T. Cederholm, P. Costelli, K. C. Fearon, A. Laviano, M. Maggio, F. Rossi Fanelli, S. M. Schneider, A. Schols, C. C. Sieber, Consensus definition of sarcopenia, cachexia and pre-cachexia: Joint document elaborated by Special Interest Groups (SIG) “cachexia-anorexia in chronic wasting diseases” and “nutrition in geriatrics”. *Clin. Nutr.* **29**, 154–159 (2010).
- S. von Haehling, S. D. Anker, Cachexia as a major underestimated and unmet medical need: Facts and numbers. *J. Cachexia. Sarcopenia Muscle* **1**, 1–5 (2010).
- K. C. H. Fearon, Cancer cachexia and fat-muscle physiology. *N. Engl. J. Med.* **365**, 565–567 (2011).
- X. Zhou, J. L. Wang, J. Lu, Y. Song, K. S. Kwak, Q. Jiao, R. Rosenfeld, Q. Chen, T. Boone, W. S. Simonet, D. L. Lacey, A. L. Goldberg, H. Q. Han, Reversal of cancer cachexia and muscle wasting by ActRIIB antagonism leads to prolonged survival. *Cell* **142**, 531–543 (2010).
- J. Huang, X. Zhu, The molecular mechanisms of calpains action on skeletal muscle atrophy. *Physiol. Res.* **65**, 547–560 (2016).
- M. Sandri, Protein breakdown in cancer cachexia. *Semin. Cell Dev. Biol.* **54**, 11–19 (2016).
- S. H. Lecker, R. T. Jagoe, A. Gilbert, M. Gomes, V. Baracos, J. Bailey, S. R. Price, W. E. Mitch, A. L. Goldberg, Multiple types of skeletal muscle atrophy involve a common program of changes in gene expression. *FASEB J.* **18**, 39–51 (2004).
- R. Sartori, G. Milan, M. Patron, C. Mammucari, B. Blaauw, R. Abraham, M. Sandri, Smad2 and 3 transcription factors control muscle mass in adulthood. *Am. J. Physiol. Cell Physiol.* **296**, C1248–C1257 (2009).
- C. E. Winbanks, K. L. Weeks, R. E. Thomson, P. V. Sepulveda, C. Beyer, H. Qian, J. L. Chen, J. M. Allen, G. I. Lancaster, M. A. Febbraio, C. A. Harrison, J. R. McMullen, J. S. Chamberlain, P. Gregorevic, Follistatin-mediated skeletal muscle hypertrophy is regulated by Smad3 and mTOR independently of myostatin. *J. Cell Biol.* **197**, 997–1008 (2012).
- C. A. Goodman, R. M. McNally, F. M. Hoffmann, T. A. Hornberger, Smad3 induces atrogen-1, inhibits mTOR and protein synthesis, and promotes muscle atrophy in vivo. *Mol. Endocrinol.* **27**, 1946–1957 (2013).
- A. Loumaye, M. de Barsey, M. Nacht, P. Lause, L. Frateur, A. van Maanen, P. Trefois, D. Gruson, J. P. Thissen, Role of activin a and myostatin in human cancer cachexia. *J. Clin. Endocrinol. Metab.* **100**, 2030–2038 (2015).
- A. Loumaye, M. de Barsey, M. Nacht, P. Lause, A. van Maanen, P. Trefois, D. Gruson, J. P. Thissen, Circulating Activin A predicts survival in cancer patients. *J. Cachexia. Sarcopenia Muscle* **8**, 768–777 (2017).
- J. L. Chen, K. L. Walton, C. E. Winbanks, K. T. Murphy, R. E. Thomson, Y. Makanji, H. Qian, G. S. Lynch, C. A. Harrison, P. Gregorevic, Elevated expression of activins promotes muscle wasting and cachexia. *FASEB J.* **28**, 1711–1723 (2014).
- K. R. Wagner, J. L. Fleckenstein, A. A. Amato, R. J. Barohn, K. Bushby, D. M. Escolar, K. M. Flanigan, A. Pestronk, R. Tawil, G. I. Wolfe, M. Eagle, J. M. Florence, W. M. King, S. Pandya, V. Straub, P. Juneau, K. Meyers, C. Csimma, T. Araujo, R. Allen, S. A. Parsons, J. M. Wozney, E. R. Lavallie, J. R. Mendell, A phase I/II trial of MYO-029 in adult subjects with muscular dystrophy. *Ann. Neurol.* **63**, 561–571 (2008).
- C. Campbell, H. J. McMillan, J. K. Mah, M. Tarnopolsky, K. Selby, T. McClure, D. M. Wilson, M. L. Sherman, D. Escolar, K. M. Attie, Myostatin inhibitor ACE-031 treatment of ambulatory boys with Duchenne muscular dystrophy: Results of a randomized, placebo-controlled clinical trial. *Muscle Nerve* **55**, 458–464 (2017).
- R. Sartori, E. Schirwis, B. Blaauw, S. Bortolanza, J. Zhao, E. Enzo, A. Stantzou, E. Mouisel, L. Toniolo, A. Ferry, S. Stricker, A. L. Goldberg, S. Dupont, S. Piccolo, H. Amthor, M. Sandri, BMP signaling controls muscle mass. *Nat. Genet.* **45**, 1309–1318 (2013).
- C. E. Winbanks, J. L. Chen, H. Qian, Y. Liu, B. C. Bernardo, C. Beyer, K. I. Watt, R. E. Thomson, T. Connor, B. J. Turner, J. R. McMullen, L. Larsson, S. L. McGee, C. A. Harrison, P. Gregorevic, The bone morphogenetic protein axis is a positive regulator of skeletal muscle mass. *J. Cell Biol.* **203**, 345–357 (2013).
- R. W. Ball, M. Warren-Paquin, K. Tsurudome, E. H. Liao, F. Elazzouzi, C. Cavanagh, B. S. An, T. T. Wang, J. H. White, A. P. Haghghi, Retrograde BMP signaling controls synaptic growth at the NMJ by regulating trio expression in motor neurons. *Neuron* **66**, 536–549 (2010).
- V. Bayat, M. Jaiswal, H. J. Bellen, The BMP signaling pathway at the Drosophila neuromuscular junction and its links to neurodegenerative diseases. *Curr. Opin. Neurobiol.* **21**, 182–188 (2011).
- S. H. Lee, Y. J. Kim, S. Y. Choi, BMP signaling modulates the probability of neurotransmitter release and readily releasable pools in Drosophila neuromuscular junction synapses. *Biochem. Biophys. Res. Commun.* **479**, 440–446 (2016).
- Y. Tanaka, H. Eda, T. Tanaka, T. Udagawa, T. Ishikawa, I. Horii, H. Ishitsuka, T. Kataoka, T. Taguchi, Experimental cancer cachexia induced by transplantable colon 26 adenocarcinoma in mice. *Cancer Res.* **50**, 2290–2295 (1990).
- G. Milan, V. Romanello, F. Pescatore, A. Armani, J. H. Paik, L. Frasson, A. Seydel, J. Zhao, R. Abraham, A. L. Goldberg, B. Blaauw, R. A. DePinho, M. Sandri, Regulation of autophagy and the ubiquitin-proteasome system by the FoxO transcriptional network during muscle atrophy. *Nat. Commun.* **6**, 6670 (2015).
- L. B. Zimmerman, J. M. De Jesus-Escobar, R. M. Harland, The Spemann organizer signal noggin binds and inactivates bone morphogenetic protein 4. *Cell* **86**, 599–606 (1996).
- C. Krause, A. Guzman, P. Knaus, Noggin. *Int. J. Biochem. Cell Biol.* **43**, 478–481 (2011).
- M. M. Matzuk, M. J. Finegold, J. P. Mather, L. Krummen, H. Lu, A. Bradley, Development of cancer cachexia-like syndrome and adrenal tumors in inhibin-deficient mice. *Proc. Natl. Acad. Sci. U.S.A.* **91**, 8817–8821 (1994).
- J. L. Chen, K. L. Walton, H. W. Qian, T. D. Colgan, A. Hagg, M. J. Watt, C. A. Harrison, P. Gregorevic, Differential effects of IL6 and activin A in the development of cancer-associated cachexia. *Cancer Res.* **76**, 5372–5382 (2016).
- S. Carnio, F. LoVerso, M. A. Baraibar, E. Longa, M. M. Khan, M. Maffei, M. Reischl, M. Canepari, S. Loeffler, H. Kern, B. Blaauw, B. Friguet, R. Bottinelli, R. Rudolf, M. Sandri, Autophagy impairment in muscle induces neuromuscular junction degeneration and precocious aging. *Cell Rep.* **8**, 1509–1521 (2014).
- X. Zhu, J. E. Yeadon, S. J. Burden, AML1 is expressed in skeletal muscle and is regulated by innervation. *Mol. Cell Biol.* **14**, 8051–8057 (1994).
- V. Moresi, A. H. Williams, E. Meadows, M. M. Flynn, M. J. Potthoff, J. McAnally, J. M. Shelton, J. Backs, W. H. Klein, J. A. Richardson, R. Bassel-Duby, E. N. Olson, Myogenin and class II HDACs control neurogenic muscle atrophy by inducing E3 ubiquitin ligases. *Cell* **143**, 35–45 (2010).
- M. Rohm, M. Schafer, V. Laurent, B. E. Ustunel, K. Niopek, C. Algire, O. Hautzinger, T. P. Sijmonsma, A. Zota, D. Medrikova, N. S. Pellegata, M. Ryden, A. Kulyte, I. Dahlman, P. Arner, N. Petrovic, B. Cannon, E. Z. Amri, B. E. Kemp, G. R. Steinberg, P. Janovska, J. Kopecky, C. Wolfrum, M. Blüher, M. Berriel Diaz, S. Herzig, An AMP-activated protein kinase-stabilizing peptide ameliorates adipose tissue wasting in cancer cachexia in mice. *Nat. Med.* **22**, 1120–1130 (2016).
- A. Rodriguez-Nuevo, A. Diaz-Ramos, E. Noguera, F. Diaz-Saez, X. Duran, J. P. Munoz, M. Romero, N. Plana, D. Sebastian, C. Tezze, V. Romanello, F. Ribas, J. Seco, E. Planet, S. R. Doctrow, J. Gonzalez, M. Borras, M. Liesa, M. Palacin, J. Vendrell, F. Villarroya, M. Sandri, O. Shirihai, A. Zorzano, Mitochondrial DNA and TLR9 drive muscle inflammation upon Opa1 deficiency. *EMBO J.* **37**, (2018).
- I. H. Jonsdottir, P. Schjerling, K. Ostrowski, S. Asp, E. A. Richter, B. K. Pedersen, Muscle contractions induce interleukin-6 mRNA production in rat skeletal muscles. *J. Physiol.* **528** (Pt. 1), 157–163 (2000).
- R. L. Starkie, M. J. Arkinstall, I. Koukoulas, J. A. Hawley, M. A. Febbraio, Carbohydrate ingestion attenuates the increase in plasma interleukin-6, but not skeletal muscle interleukin-6 mRNA, during exercise in humans. *J. Physiol.* **533**, 585–591 (2011).
- A. Bonetto, T. Aydogdu, N. Kunzevitzky, D. C. Guttridge, S. Khuri, L. G. Koniaris, T. A. Zimmers, STAT3 activation in skeletal muscle links muscle wasting and the acute phase response in cancer cachexia. *PLOS ONE* **6**, e22538 (2011).
- B. J. Caan, J. A. Meyerhardt, C. H. Kroenke, S. Alexeeff, J. Xiao, E. Weltzien, E. C. Feliciano, A. L. Castillo, C. P. Quesenberry, M. L. Kwan, C. M. Prado, Explaining the obesity paradox: The association between body composition and colorectal cancer survival (C-SCANS Study). *Cancer Epidemiol. Biomarkers Prev.* **26**, 1008–1015 (2017).
- M. VanSaun, M. J. Werle, Matrix metalloproteinase-3 removes agrin from synaptic basal lamina. *J. Neurobiol.* **44**, 369 (2000).
- S. Hettwer, P. Dahinden, S. Kucsera, C. Farina, S. Ahmed, R. Fariello, M. Drey, C. C. Sieber, J. W. Vrijbloed, Elevated levels of a C-terminal agrin fragment identifies a new subset of sarcopenia patients. *Exp. Gerontol.* **48**, 69–75 (2013).
- M. Drey, C. C. Sieber, J. M. Bauer, W. Uter, P. Dahinden, R. G. Fariello, J. W. Vrijbloed; FiAT intervention group, C-terminal agrin fragment as a potential marker for sarcopenia caused by degeneration of the neuromuscular junction. *Exp. Gerontol.* **48**, 76–80 (2013).
- A. Niezgodá, S. Michalak, J. Losy, A. Kalinowska-Lyszczarz, W. Kozubski, sNCAM as a specific marker of peripheral demyelination. *Immunol. Lett.* **185**, 93–97 (2017).
- H. An, L. Zhou, Y. Yu, H. Fan, F. Fan, S. Tan, Z. Wang, B. Z, J. Shi, F. Yang, X. Zhang, Y. Tan, X. F. Huang, Serum NCAM levels and cognitive deficits in first episode schizophrenia patients versus health controls. *Schizophr. Res.* **192**, 457–458 (2018).
- A. Anoveros-Barrera, A. S. Bhullar, C. Stretch, N. Esfandiari, A. R. Dunichand-Hoeld, K. J. B. Martins, D. Bigam, R. G. Khadaroo, T. McMullen, O. F. Bathe, S. Damaraju, R. J. Skipworth, C. T. Putman, V. E. Baracos, V. C. Mazurak, Clinical and biological characterization of skeletal muscle tissue biopsies of surgical cancer patients. *J. Cachexia. Sarcopenia Muscle* **10**, 1356–1377 (2019).
- V. Dubowitz, C. A. Sewry, R. B. Fitzsimons, in *Muscle Biopsy: A Practical Approach* (Baillière Tindall, 1985), pp. 19–40
- J. L. Andersen, Muscle fibre type adaptation in the elderly human muscle. *Scand. J. Med. Sci. Sports* **13**, 40–47 (2003).
- S. Mosole, U. Carraro, H. Kern, S. Loeffler, H. Fruhmann, M. Vogelauer, S. Burggraf, W. Mayr, M. Krenn, T. Paternostro-Sluga, D. Hamar, J. Cvecka, M. Sedliak, V. Tirkpova, N. Sarabon,

- A. Musaro, M. Sandri, F. Protasi, A. Nori, A. Pond, S. Zampieri, Long-term high-level exercise promotes muscle reinnervation with age. *J. Neuropathol. Exp. Neurol.* **73**, 284–294 (2014).
46. O. Lepparanta, J. M. Tikkanen, M. M. Bupalov, K. Koli, M. Myllarniemi, Bone morphogenetic protein-inducer tilorone identified by high-throughput screening is antifibrotic in vivo. *Am. J. Respir. Cell Mol. Biol.* **48**, 448–455 (2013).
47. S. Aykul, E. Martinez-Hackert, Transforming growth factor- $\beta$  family ligands can function as antagonists by competing for type II receptor binding. *J. Biol. Chem.* **291**, 10792–10804 (2016).
48. V. Banduseela, J. Ochala, K. Lamberg, H. Kalimo, L. Larsson, Muscle paralysis and myosin loss in a patient with cancer cachexia. *Acta Myol.* **26**, 136–144 (2007).
49. M. K. Rubinstein, Carcinomatous neuromyopathy. The non-metastatic effects of cancer on the nervous system. *Calif. Med.* **110**, 482–492 (1969).
50. D. S. Chandrashekar, B. Bachel, S. A. H. Balasubramanya, C. J. Creighton, I. Ponce-Rodriguez, B. V. S. K. Chakravarthi, S. Varambally, UALCAN: A portal for facilitating tumor subgroup gene expression and survival analyses. *Neoplasia* **19**, 649–658 (2017).
51. Cancer Genome Atlas Research Network, Integrated genomic characterization of pancreatic ductal adenocarcinoma. *Cancer Cell* **32**, 185–203.e13 (2017).
52. Cancer Genome Atlas Research Network, Comprehensive molecular characterization of human colon and rectal cancer. *Nature* **487**, 330–337 (2012).
53. E. E. Talbert, M. C. Cuitiño, K. J. Ladner, P. V. Rajasekera, M. Siebert, R. Shakya, G. W. Leone, M. C. Ostrowski, B. Paleo, N. Weisleder, P. J. Reiser, A. Webb, C. D. Timmers, D. S. Eiferman, D. C. Evans, M. E. Dillhoff, C. R. Schmidt, D. C. Guttridge, Modeling human cancer-induced cachexia. *Cell Rep.* **28**, 1612–1622.e4 (2019).
54. M. Sandri, C. Sandri, A. Gilbert, C. Skurk, E. Calabria, A. Picard, K. Walsh, S. Schiaffino, S. H. Lecker, A. L. Goldberg, Foxo transcription factors induce the atrophy-related ubiquitin ligase atrogin-1 and cause skeletal muscle atrophy. *Cell* **117**, 399–412 (2004).
55. C. E. Winbanks, K. T. Murphy, B. C. Bernardo, H. Qian, Y. Liu, P. V. Sepulveda, C. Beyer, A. Hagg, R. E. Thomson, J. L. Chen, K. L. Walton, K. L. Loveland, J. R. McMullen, B. D. Rodgers, C. A. Harrison, G. S. Lynch, P. Gregorevic, *Smad7* gene delivery prevents muscle wasting associated with cancer cachexia in mice. *Sci. Transl. Med.* **8**, 348ra98 (2016).
56. P. Aulino, E. Berardi, V. M. Cardillo, E. Rizzuto, B. Perniconi, C. Ramina, F. Padula, E. P. Spugnini, A. Baldi, F. Faiola, S. Adamo, D. Coletti, Molecular, cellular and physiological characterization of the cancer cachexia-inducing C26 colon carcinoma in mouse. *BMC Cancer* **10**, 363 (2010).
57. F. Penna, D. Costamagna, F. Pin, A. Camperi, A. Fanzani, E. M. Chiarpotto, G. Cavallini, G. Bonelli, F. M. Baccino, P. Costelli, Autophagic degradation contributes to muscle wasting in cancer cachexia. *Am. J. Pathol.* **182**, 1367–1378 (2013).
58. M. Di Bari, L. V. van de Poll-Franse, G. Onder, S. B. Kritchevsky, A. Newman, T. B. Harris, J. D. Williamson, N. Marchionni, M. Pahor, Antihypertensive medications and differences in muscle mass in older persons: The health, aging and body composition study. *J. Am. Geriatr. Soc.* **52**, 961–966 (2004).
59. T. N. Burks, E. Andres-Mateos, R. Marx, R. Mejias, C. Van Erp, J. L. Simmers, J. D. Walston, C. W. Ward, R. D. Cohn, Losartan restores skeletal muscle remodeling and protects against disuse atrophy in sarcopenia. *Sci. Transl. Med.* **3**, 82ra37 (2011).
60. P. Delafontaine, T. Yoshida, The renin-angiotensin system and the biology of skeletal muscle: Mechanisms of muscle wasting in chronic disease states. *Trans. Am. Clin. Climatol. Assoc.* **127**, 245–258 (2016).
61. J. Boutbir, F. Singh, A. L. Charles, A. I. Schlagowski, A. Bonifacio, A. Echaniz-Laguna, B. Geny, S. Krahenbuhl, J. Zoll, Statins trigger mitochondrial reactive oxygen species-induced apoptosis in glycolytic skeletal muscle. *Antioxid. Redox Signal.* **24**, 84–98 (2016).
62. P. S. Phillips, R. H. Haas, S. Bannykh, S. Hathaway, N. L. Gray, B. J. Kimura, G. D. Vladutiu, J. D. F. England, Scripps Mercy Clinical Research Center, Statin-associated myopathy with normal creatine kinase levels. *Ann. Intern. Med.* **137**, 581–585 (2002).
63. R. A. Standley, S. Z. Liu, B. Jemiolo, S. W. Trappe, T. A. Trappe, Prostaglandin E2 induces transcription of skeletal muscle mass regulators interleukin-6 and muscle RING finger-1 in humans. *Prostaglandins Leukot. Essent. Fatty Acids* **88**, 361–364 (2013).
64. S. Z. Liu, B. Jemiolo, K. M. Lavin, B. E. Lester, S. W. Trappe, T. A. Trappe, Prostaglandin E<sub>2</sub> cyclooxygenase pathway in human skeletal muscle: Influence of muscle fiber type and age. *J. Appl. Physiol.* **120**, 546–551 (2016).
65. U. Ferrari, C. Then, M. Rottenkolber, C. Selte, J. Seissler, R. Conzade, B. Linkohr, A. Peters, M. Drey, B. Thorand, Longitudinal association of type 2 diabetes and insulin therapy with muscle parameters in the KORA-Age study. *Acta Diabetol.* **57**, 1057–1063 (2020).
66. F. F. Bloise, T. S. Oliveira, A. Cordeiro, T. M. Ortega-Carvalho, Thyroid hormones play role in sarcopenia and myopathies. *Front. Physiol.* **9**, 560 (2018).
67. D. Salvatore, W. S. Simonides, M. Dentice, A. M. Zavacki, P. R. Larsen, Thyroid hormones and skeletal muscle—New insights and potential implications. *Nat. Rev. Endocrinol.* **10**, 206–214 (2014).
68. S. K. Malin, S. R. Kashyap, Effects of metformin on weight loss: Potential mechanisms. *Curr. Opin. Endocrinol. Diabetes Obes.* **21**, 323–329 (2014).
69. B. Wessels, J. Ciapaite, N. M. van den Broek, K. Nicolay, J. J. Prompers, Metformin impairs mitochondrial function in skeletal muscle of both lean and diabetic rats in a dose-dependent manner. *PLOS ONE* **9**, e100525 (2014).
70. O. Elsaid, B. Taylor, A. Zaleski, G. Panza, P. D. Thompson, Rationale for investigating metformin as a protectant against statin-associated muscle symptoms. *J. Clin. Lipidol.* **11**, 1145–1151 (2017).
71. F. Derbre, B. Ferrando, M. C. Gomez-Cabrera, F. Sanchis-Gomar, V. E. Martinez-Bello, G. Olaso-Gonzalez, A. Diaz, A. Gratas-Delamarche, M. Cerda, J. Vina, Inhibition of xanthine oxidase by allopurinol prevents skeletal muscle atrophy: Role of p38 MAPKinase and E3 ubiquitin ligases. *PLOS ONE* **7**, e46668 (2012).
72. S. C. Bodine, J. D. Furlow, Glucocorticoids and skeletal muscle. *Adv. Exp. Med. Biol.* **872**, 145–176 (2015).
73. O. Schakman, S. Kalista, C. Barbe, A. Loumaye, J. P. Thissen, Glucocorticoid-induced skeletal muscle atrophy. *Int. J. Biochem. Cell Biol.* **45**, 2163–2172 (2013).
74. C. Vuong, S. H. Van Uum, L. E. O'Dell, K. Lutfy, T. C. Friedman, The effects of opioids and opioid analogs on animal and human endocrine systems. *Endocr. Rev.* **31**, 98–132 (2010).
75. P. Anagnostis, N. K. Gkekas, C. Achilla, G. Pananastasiou, P. Taoukidou, M. Mitsiou, E. Kenanidis, M. Potoupnis, E. Tsiridis, D. G. Goulis, Type 2 diabetes mellitus is associated with increased risk of sarcopenia: A systematic review and meta-analysis. *Calif. Tissue Int.* **107**, 453–463 (2020).
76. H. Triewweiler, G. Kislewicz, T. Hoffmann Jonasson, R. Rasmussen Petherle, C. Aguiar Moreira, V. Zeghibi Cochenski Borba, Sarcopenia: A chronic complication of type 2 diabetes mellitus. *Diabetol. Metab. Syndr.* **10**, 25 (2018).
77. R. C. J. Langen, H. R. Gosker, A. H. V. Remels, A. M. W. J. Schols, Triggers and mechanisms of skeletal muscle wasting in chronic obstructive pulmonary disease. *Int. J. Biochem. Cell Biol.* **45**, 2245–2256 (2013).
78. R. C. I. Wüst, H. Degens, Factors contributing to muscle wasting and dysfunction in COPD patients. *Int. J. Chron. Obstruct. Pulmon. Dis.* **2**, 289–300 (2007).
79. V. A. de Souza, D. Oliveira, S. R. Barbosa, J. O. d. A. Corrêa, F. A. B. Colugnati, H. N. Mansur, N. M. d. S. Fernandes, M. G. Bastos, Sarcopenia in patients with chronic kidney disease not yet on dialysis: Analysis of the prevalence and associated factors. *PLOS ONE* **12**, e0176230 (2017).
80. M. Mourtzakis, C. M. M. Prado, J. R. Lieffers, T. Reiman, L. J. McCargar, V. E. Baracos, A practical and precise approach to quantification of body composition in cancer patients using computed tomography images acquired during routine care. *Appl. Physiol. Nutr. Metab.* **33**, 997–1006 (2008).
81. S. B. Heymsfield, D. Gallagher, M. Visser, C. Nuñez, Z. M. Wang, Measurement of skeletal muscle: Laboratory and epidemiological methods. *J. Gerontol. A Biol. Sci. Med. Sci.* **50**, 23–29 (1995).
82. A. J. MacDonald, C. A. Greig, V. Baracos, The advantages and limitations of cross-sectional body composition analysis. *Curr. Opin. Support. Palliat. Care* **5**, 342–349 (2011).
83. O. Korchynskyi, P. ten Dijke, Identification and functional characterization of distinct critically important bone morphogenetic protein-specific response elements in the Id1 promoter. *J. Biol. Chem.* **277**, 4883–4891 (2002).
84. O. Rossetto, L. Gorza, G. Schiavo, N. Schiavo, R. H. Scheller, C. Montecucco, VAMP/synaptobrevin isoforms 1 and 2 are widely and differentially expressed in nonneuronal tissues. *J. Cell Biol.* **132**, 167–179 (1996).
85. G. Schiavo, C. C. Shone, M. K. Bennett, R. H. Scheller, C. Montecucco, Botulinum neurotoxin type C cleaves a single Lys-Ala bond within the carboxyl-terminal region of syntaxins. *J. Biol. Chem.* **270**, 10566–10570 (1995).
86. M. J. Blankinship, P. Gregorevic, J. M. Allen, S. Q. Harper, H. Harper, C. L. Halbert, D. A. Miller, J. S. Chamberlain, Efficient transduction of skeletal muscle using vectors based on adeno-associated virus serotype 6. *Mol. Ther.* **10**, 671–678 (2004).
87. J. N. Sleight, R. W. Burgess, T. H. Gillingwater, M. Z. Cader, Morphological analysis of neuromuscular junction development and degeneration in rodent lumbrical muscles. *J. Neurosci. Methods* **227**, 159–165 (2014).
88. E. Duregotti, G. Zanetti, M. Scorzeto, A. Megighian, C. Montecucco, M. Pirazzini, M. Rigoni, Snake and spider toxins induce a rapid recovery of function of botulinum neurotoxin paralysed neuromuscular junction. *Toxins* **7**, 5322–5336 (2015).
89. C. E. Winbanks, B. Wang, C. Beyer, P. Koh, L. White, P. Kantharidis, P. Gregorevic, TGF- $\beta$  regulates miR-206 and miR-29 to control myogenic differentiation through regulation of HDAC4. *J. Biol. Chem.* **286**, 13805–13814 (2011).
90. S. A. Polyzos, J. Kountouras, A. D. Anastasilakis, P. Makras, G. Hawa, L. Sonnleitner, A. Missbichler, M. Doulberis, P. Katsinelos, E. Terpos, Noggin levels in nonalcoholic fatty liver disease: The effect of vitamin E treatment. *Hormones* **17**, 573–579 (2018).
91. U. Carraro, D. Morale, I. Mussini, S. Lucke, M. Cantini, R. Betto, C. Catani, L. Dalla Libera, D. Danielli Betto, D. Noventa, Chronic denervation of rat hemidiaphragm: Maintenance of fiber heterogeneity with associated increasing uniformity of myosin isoforms. *J. Cell Biol.* **100**, 161–174 (1985).

92. F. G. I. Jennekens, B. E. Tomlinson, J. N. Walton, Histochemical aspects of five limb muscles in old age An autopsy study. *J. Neurol. Sci.* **14**, 259–276 (1971).

**Acknowledgments:** We are grateful to the patients who participated in this study. We thank Monash Micro Imaging staff, AMREP campus, and the Biological Optical Microscopy Platform, The University of Melbourne for technical guidance; S. Jansen and AMREP Precinct Animal Centre staff for animal husbandry and technical assistance; C. A. Goodman for technical advice; and M. Forster, F. Cavallin, S. Zumerle, and S. Cecchinello for valuable help. Noggin protein concentrations in muscle lysates were determined by G. Hawa (Fianostics GmbH, Wiener Neustadt, Austria). Inhibin- $\alpha^{+/}$  mice were a gift from M. M. Matzuk (Baylor College of Medicine). MC38 cells were a gift from I. Marigo (Istituto Oncologico Veneto, IOV-IRCCS). Antibodies targeting VAMP1 and Syntaxin IA/IB were provided as a gift from the laboratory of C. Montecucco (University of Padova). The antibody targeting phosphorylated SMAD1 was a gift from P. ten Dijke (Leiden University Medical Centrum of Netherlands). **Funding:** Studies were supported by a project grant (1121500 awarded to P.G. and L.L.) from the National Health and Medical Research Council of Australia (NHMRC), an international collaboration project from the Swedish Foundation for International Co-operation in Research and Higher Education (STINT) awarded to L.L. and P.G., an Endeavour Research Fellowship from the Department of Education and Training, Australian Government to R.S., two postdoctoral fellowships from Fondazione Umberto Veronesi (ID2496 and ID3519 to R.S.) and a postdoctoral fellowship from the Association Française Contre les Myopathies (AFM-Téléthon, ID21938 awarded to R.S.), funding awarded by the Italian Association for Cancer Research (AIRC IG - ID17388 and ID23257), ASI (MARS-PRE, project no DC-VUM-2017-006), and H2020-MSCA-RISE-2014 project no. 645648 “Muscle Stress Relief” awarded to M.S., funding awarded by the Italian Association for Cancer Research (AIRC IG 2018—ID.21963 project awarded to F.P.), project funding from the Stafford Fox Medical Research Foundation to awarded B.J.T., an Australian Post Graduate Award (Department of Education and Training,

Australian Government), a PhD stipend top-up award from the Baker Heart and Diabetes Institute Bright Sparks program awarded to A.H., and a Senior Research Fellowship (1117835, NHMRC, Australia) awarded to P.G. The Baker Heart and Diabetes Institute is supported, in part, by an operational infrastructure support program from the Victorian Government.

**Author contributions:** Conceptualization: R.S., A.H., C.E.W., K.I.W., M.V., F.P., M.S., and P.G. Investigation: R.S., A.H., C.E.W., A.A., S.Z., L.R.V., K.I.W., M.H., P.Z., C.P., M.K., F.P., A.M., A.L., R.E.T., and P.G. Resources: R.S., F.P., S.Z., H.Q., B.J.T., G.Z., E.S.P., L.M., M.V., G.D.D., C.S., L.L., K.L.L., P.C., S.M., M.S., and P.G. Validation: R.S., A.H., C.E.W., S.Z., A.A., F.P., B.J.T., M.S., and P.G. Formal analysis: R.S., A.H., C.E.W., K.I.W., S.Z., M.H., A.A., A.P., S.A., F.P., B.J.T., M.S., and P.G. Writing—original draft: R.S., A.H., M.S., and P.G. Supervision: R.S., F.P., M.S., and P.G. Funding acquisition: M.S., L.L., and P.G. All authors reviewed the manuscript before submission. **Competing interests:** The authors declare that they have no competing financial interests. **Data and materials availability:** All data needed to evaluate the conclusions in the paper are present in the paper and/or the Supplementary Materials.

Submitted 1 August 2019

Accepted 18 March 2021

Published 4 August 2021

10.1126/scitranslmed.aay9592

**Citation:** R. Sartori, A. Hagg, S. Zampieri, A. Armani, C. E. Winbanks, L. R. Viana, M. Haidar, K. I. Watt, H. Qian, C. Pezzini, P. Zanganeh, B. J. Turner, A. Larsson, G. Zanchettin, E. S. Pierobon, L. Moletta, M. Valmasoni, A. Ponzoni, S. Attar, G. Da Dalt, C. Sperti, M. Kustermann, R. E. Thomson, L. Larsson, K. L. Loveland, P. Costelli, A. Megighian, S. Merigliano, F. Penna, P. Gregorevic, M. Sandri, Perturbed BMP signaling and denervation promote muscle wasting in cancer cachexia. *Sci. Transl. Med.* **13**, eaay9592 (2021).

## Perturbed BMP signaling and denervation promote muscle wasting in cancer cachexia

Roberta Sartori, Adam Hagg, Sandra Zampieri, Andrea Armani, Catherine E. Winbanks, Las R. Viana, Mouna Haidar, Kevin I. Watt, Hongwei Qian, Camilla Pezzini, Pardis Zanganeh, Bradley J. Turner, Anna Larsson, Gianpietro Zanchettin, Elisa S. Pierobon, Lucia Moletta, Michele Valmasoni, Alberto Ponzoni, Shady Attar, Gianfranco Da Dalt, Cosimo Sperti, Monika Kustermann, Rachel E. Thomson, Lars Larsson, Kate L. Loveland, Paola Costelli, Aram Megighian, Stefano Merigliano, Fabio Penna, Paul Gregorevic, and Marco Sandri

*Sci. Transl. Med.*, **13** (605), eaay9592.  
DOI: 10.1126/scitranslmed.aay9592

### Reducing waste

Cancer is often associated with the development of cachexia, a severe muscle wasting process for which there are no specific therapies. The precise mechanisms and the molecular players involved in cancer-associated muscle wasting remain to be identified. Here, Sartori *et al.* showed that bone morphogenetic protein (BMP) was reduced in patients and rodent models. This reduction caused neuromuscular junction impairments and subsequent denervation that caused muscle mass reduction. Restoring BMP signaling preserved muscles and increased survival in tumor-bearing mice, suggesting that restoring muscle mass by targeting BMP could be effective for improving life quality and life span in patients with cancer.

### View the article online

<https://www.science.org/doi/10.1126/scitranslmed.aay9592>

### Permissions

<https://www.science.org/help/reprints-and-permissions>

Use of this article is subject to the [Terms of service](#)